REMARKS/ARGUMENTS

Claims 1, 3, 5, 11, 15, 16 and 39-42 are active in this application. No new subject matter has been added from the amended and the new claims. Claim 1 is supported in pages 4-7, page 19, figures 1 and 4 of the specification as originally filed. Claim 39 is supported at paragraph [0061], [0064] and [0065] in the specification. Claim 40 is supported by Example 10. Claim 41 is supported by example 11. Claim 42 is supported at paragraph [0031] in the specification. No new matter is believed to be added.

As discussed in the present specification, TREM 1 is a receptor of activation in macrophages. TREM 1 includes a soluble extracellular domain and a hydrophobic transmembrane domain (see Fig. 1) that when triggered by its ligand, the ligated complex induces macrophage activation. TREM 1-SV is a variant of TREM-1 that is not anchored in the macrophage cell membrane but free to capture TREM-1 ligand. When TREM-1 ligand is captured by TREM 1-SV the TREM-1 receptor complex is not triggered and the macrophages are not activated. Depending at what stage of the condition or disease the intervention is practiced, this permits the modulation (down and up activation) of the immune response. For instance, if the TREM-1sv treatment is repeatedly practiced as a prophylactic intervention and then the patient develops an infection, one skilled in the art knows to reduce the treatment to allow the immune response to activate gradually to fight the infection without overdoing it and going into septic shock.

In view of these comments, the claim amendments submitted, and the following remarks, Applicants request reconsideration of all outstanding rejections.

The new matter rejection pertaining to Claims 1, 3, 5, 7, 9, and 11-16 under 35 U.S.C. § 112, first paragraph is not deemed to be applicable in light of the amendments submitted herein. Specifically, while Applicants disagree with the Examiner's interpretation of the specification, the language in the claims that was the basis for the rejection is no longer

present. Rather, the polypeptide used in the claimed methods is defined by having a portion of the sequence in SEQ ID NO:2, which is clearly described, e.g. in the sequence itself presented in Figure 4. Withdrawal of this ground of rejection is requested.

The rejection of Claims 1, 3, 5, 7, 9, and 11-16 under 35 U.S.C. 112, first paragraph ("enablement") is respectfully traversed.

The scope of this rejection summarizes as this application having a lack of description in the specifications about the method to modulate the immune response by competitive inhibition with a soluble TREM-1 or one without a functional transmembrane region. Applicants have amended the claims to clarify that the scope of this patent resides in the therapeutic action of the binding ligand activity of the compound and not whether it has a functional transmembrane region or not. The binding ligand region or site of activity of the compound claimed is described in Figure 4 and paragraph [0027] as being the region from one box to another inclusively, the two boxes being described as containing the sequence where the disulfide bridges originates . A schematic presentation of the loop binding domain is presented in Figure 1 and described in paragraph [0024]. The functionality of the structure of TREM-1sv is known based on its gene location and its similarity with the immunoglobulins and T cell receptor family. A pair of disulfide bridges creates a loop domain or binding domain that contains the binding sites for this type of immunoglobulin family.related receptors (see the present specification at paragraph [0070] and Kelker et al. *J. Mol. Biol.* 342:1237, 2004, copy attached).

Furthermore, Applicants point out that:

1. The mechanisms by which the polypeptide competes for the TREM-1 ligand is described thoughout the specification. Modulation of this mechanism is inherent to its property.

2. The structure of different TREM-1 molecules across species have been studied and regardless of their transmembrane region, their ligand binding site is a common conservative region forming a loop binding domain created by a pair of disulfides bridges, one on each end of the loop. Applicants point to the attached publications Kelker et al. *J. Mol. Biol.* 342:1237, 2004 and Ibid. *J. Mol. Biol.* 344:1175, 2004 in support of these statements.

3. The enablement of the claimed therapeutic action of the composition having this binding ligand activity is supported by the data in Bouchon et al., *Nature* 410:1103, 2001, and Gibot et al., J Exp Med. 200:1419, 2004. The assumption of the examiner that a difference in the transmembrane region could jeopardize the therapeutic activity of the ligand binding sites does not have any supporting data in light of Kelker et al. studies mentioned above in 2., showing a common loop of binding sites to all TREM-1 molecules and in view of Gibot et al., *J Exp Med.* 200:1419, 2004 whom created only a small peptide bearing binding ligand activity and in view of Bouchon et al., *Nature* 410:1103, 2001 whom created a soluble TREM-1. In both cases, as long as the binding sites are present there is binding ligand activity and thus a therapeutic action.

4. One can practice the claimed invention because one can predict the therapeutic efficacy of the composition with TREM-1 ligand activity as long as it contains a portion of the TREM-1SV (see amino acids 1-136 of SEQ ID NO:2) that provides a therapeutic action.

5. One skill in the art can practice this invention based on the competitive inhibition, neutralization or enhancement mechanisms described in the specifications and in the art as practiced by Bouchon et al., *Nature* 410:1103, 2001, and Gibot et al., *J Exp Med.* 200:1419, 2004.

6. The sequence of the ligand binding site and the generation of a polypeptide for application use for therapy is well disclosed in this application. A person skilled in the art can find all the means to practice this invention to obtain a therapeutic action.

In light of the above, the claims are enabled and respectfully request that the rejection be withdrawn.

The rejection of Claims 1, 3, 5, 7, 9 and 11-16 under 35 U.S.C. 102 (e) in view of US Patent 6,420,526 or US Patent 6,504,010 is respectfully traversed. .

At the outset, one might ask why, since 1952, the patent statutes have specifically permitted the patenting of a new use for an "old process . . . composition of matter or material. (See 35 U.S.C. § 100(b)). Surely, an old process or composition of matter is already in the public domain. Yet, Congress deliberately chose to include as patentable subject matter the new use of an old process or composition of matter. One reason for this is the desire of our society to foster investigation of old processes and materials to find new uses therefor.

There is no evidence of record that prior to Applicants' work, those skilled in the art targeted the ligand binding activity of TREM-1 to modulate immune responses in patients or even test animals. One must consider now many lives can be saved by knowing that such a composition may be used to treat immune conditions such as autoimmune diseases and septic shock.

The Examiner should recognize that before a corporation can contemplate suggesting the use, commercially, of the composition as claimed for the purpose of modulating immune responses, it is quite likely that the corporation selling the composition for that purpose would seek Food and Drug approval for the new use. Obtaining Food and Drug approval is an extremely expensive process. Accordingly, absent the grant of a patent, or some form of exclusivity, a corporation would be naturally reluctant to expend the funds necessary to develop the new use invention and obtain FDA approval since there will be no way of recouping the investment.

Accordingly, the Congress saw fit to enact legislation which permits obtaining patents for new uses of old processes and compositions because the grant of the patent serves to stimulate research and development and to bring valuable, potentially life saving, products to market.

Applicants' claims direct the invention specifically to the new use (method) of modulating immune function in a patient. Indeed, amended Claim 1 is concerned with the new use of modulating immune response.

US Patent 6,504,010 describes a several hundred sequences, one of which is similar to TREM-1sv strictly for the purpose of treating cancer, generally and lung cancer, specifically.

US Patent 6,420,526 is very vague patent. The '526 patent describes a sequence with no details in the specifications on which sequence of the molecule has a function. Functions are associated with translated proteins not with a EST DNA sequence. US Patent 6,420,526 is a multiple EST sequence patent (186 all together) containing the sequence 159 that is the subject of this objection. Sequence 159 contains 6 paragraphs for a total of a little over one page. The description in patent 526 suggests a potential use to regulate the immune response but does not describe enough to reduce to practice without undue experiments such as which part of the molecule is relevant to practice the invention. To the contrary of our application, patent 526 description is 1) minimal with a lack of description on the molecule to use and its functional sites for someone to reduce this invention to practice. 2) There is no guidance or working evidence presented to support the rejection.

The Federal Circuit's decision in *Jansen v. Rexall Sundown Inc.,* 68 U.S.P.Q.2d 1154 (Fed. Cir. 2003) resolves the prior art issues in this case and requires that the currently pending prior art rejections be withdrawn.

In *Jansen*, the claims were directed to methods of treating or preventing macrocytic-megaloblastic anemia comprising administering effective amounts of folic acid and vitamin

B_{12} to humans in need thereof. *Jansen* at 1157. In interpreting these claims, the Federal Circuit ruled that the claims require the specific intent to achieve the claimed objective (treatment or prevention of macrocytic-megaloblastic anemia). Specifically, the Federal Circuit stated that:

> . . . the claim preamble sets forth the objective of the method, and the body of the claim directs that the method be performed on someone 'in need.' In both cases, the claims' recitation of a patient or a human 'in need' gives life and meaning to preambles. [Citation omitted]. The preamble is therefore not merely a statement of effect that may or may not be desired or appreciated. Rather, **it is a statement of the intentional purpose for which the method must be performed**. We need not decide whether we would reach the same conclusion if either of the 'treating or preventing' phrase or the 'to a human in need thereof' phrase was not a part of the claim; **together, however, they compel the claim construction arrived at by both the district court and this court**.

Jansen at 1158 (emphasis added). The Federal Circuit further explained that:

> the '083 patent claims are properly interpreted to mean that the combination of folic acid and vitamin B_{12} **must** be administered to a human with a recognized need to treat or prevent macrocytic-megaloblastic anemia.

Jansen at 1158 (emphasis added).

Thus, according to the Federal Circuit, claims directed to methods of treatment to be performed on those in need of such treatment require the specific intent to effect such treatment.

In the present application, the pending claims are directed to methods of modulating immune response in an animal in need thereof by administering a composition in an amount effective to modulate TREM 1SV ligand binding activity. In accordance with the Federal

Circuit's decision in *Jansen*, these claims must be interpreted to require the specific intent to effect such immuno-modulatory activities.

None of the cited art teaches or suggests such specific intent: that is, none of the prior art states that the composition, including a portion of SEQ ID NO:2 should be used in this manner. Moreover, none of the prior art constitutes a polypeptide or polypeptide mimetic-containing product for which advertisements, instructions and/or directions relate to modulating immune response as claimed. In view of such fatal deficiencies, the prior art cannot teach or suggest the claimed methods.

To the Examiner's belief that the prior art inherently resulted in the claimed methods, thereby rendering such methods unpatentable, such an inherency argument is inapplicable in this case.

In *Jansen*, the Federal Circuit discussed its earlier decision in *Rapoport v. Dement*, 254 F.3d 1053 (Fed. Cir. 2001) (copy enclosed). In *Rapoport*, the claims were directed to methods of treating sleep apneas comprising administering an effective amount of an azapirone compound to a patient in need of such treatment. In *Jansen*, the Federal Circuit characterized its *Rapoport* decision as follows:

> We rejected [the argument that prior art disclosing treatment of a symptom of sleep apnea actually disclosed treatment of sleep apnea in *Rapoport*], stating, 'There is no disclosure in the [prior art reference that the compound] is administered to patients suffering from sleep apnea *with the intent to cure the underlying condition.*' Thus, the claim was interpreted to require that the method be practiced with the intent to achieve the objective stated in the preamble.

Jansen at 1157 (emphasis in original).

In *Rapoport*, the Federal Circuit addressed the issue of inherency (that is, whether prior art related to treating symptoms of sleep apnea inherently anticipated the claimed

methods of treating sleep apnea). The Federal Circuit rejected this argument on two independent grounds.

First, and most importantly, the Federal Circuit noted that prior art did not disclose administering the compound to patients suffering from sleep apnea. *Rapoport* at 1062. Thus, as noted in *Jansen*, the prior art did not disclose administering the compound to patients suffering from sleep apnea "*with the intent to cure the underlying condition.*" Similarly, prior art which does not disclose utilizing a composition including a polypeptide or mimetic in an amount sufficient to modulate TREM-1SV ligand binding activity cannot inherently anticipate or render obvious the claimed invention. For this reason alone the prior art rejections are improper and should be withdrawn.

The second independent ground was that it had not been demonstrated that the prior art regimen would necessarily result in treating sleep apnea even assuming such a regimen were administered to one suffering from sleep apnea. *Rapoport* at 1062-63. Similarly, and as set forth above, reproducing the cited prior art in this case would not necessarily result in practicing the claimed methods. For this reason as well the prior art does not inherently anticipate or render obvious the claimed invention.

In view of the above, Applicant respectfully requests that the rejections under 35 U.S.C. § 102 be withdrawn.

In view of the above, each of the presently pending claims in this application is believed to be in immediate condition for allowance. Accordingly, the Examiner is respectfully requested to pass this application to issue.

Respectfully submitted,

OBLON, SPIVAK, McCLELLAND,
MAIER & NEUSTADT, P.C.
Norman F. Oblon

Daniel J. Pereira, Ph.D.
Registration No. 45,518

Customer Number
22850

Tel: (703) 413-3000
Fax: (703) 413 -2220
(OSMMN 06/04)

doi:10.1016/j.jmb.2004.10.009 J. Mol. Biol. (2004) 344, 1175–1181

JMB Available online at www.sciencedirect.com SCIENCE DIRECT® ELSEVIER

COMMUNICATION

Crystal Structure of Mouse Triggering Receptor Expressed on Myeloid Cells 1 (TREM-1) at 1.76 Å

Matthew S. Kelker, Erik W. Debler and Ian A. Wilson*

Department of Molecular Biology and The Skaggs Institute for Chemical Biology The Scripps Research Institute La Jolla, CA 92037, USA

*Corresponding author

Triggering receptor expressed on myeloid cells (TREM) 1 is an activating receptor expressed on myeloid cells whose ligand(s) remain elusive. TREM-1 stimulation activates neutrophils and monocytes and induces the secretion of pro-inflammatory molecules, which amplifies the Toll-like receptor-initiated responses to invading pathogens. In addition, TREM-1 mediates the septic shock pathway, and thus represents a potential therapeutic target. We report the crystal structure of the mouse TREM-1 extracellular domain at 1.76 Å resolution. The mouse extracellular domain is monomeric, consistent with our previous human TREM-1 structure, and strongly supports the contention that the globular TREM-1 head is a monomer contrary to proposals of a symmetric dimer.

Keywords: crystal structure; activating receptors; TREM-1; innate immunity; immune system receptor

The adaptive immune system is an antigen-driven and antigen-specific system whose germline-encoded receptors undergo further editing and processing *via* clonal selection and expansion. Conversely, the innate immune system is comprised of germline-encoded, generic antigen receptors, which represent the first line of defense against invading pathogens. A family of such receptors expressed on myeloid cells, termed triggering receptor expressed on myeloid cells (TREMs) has been described,[1,2] and one of them, TREM-1, is an important link between the innate and adaptive systems.[3] TREMs amplify a pathway involved in mediating the inflammatory response to microbial products; however, they lack direct signaling capabilities and must associate with the signaling molecule DAP12.[4] TREM-1 stimulation with lipopolysaccharides (LPS), activates neutrophils and monocytes, and induces the secretion of pro-inflammatory chemokines, cytokines and adhesion molecules. Excessive release of such molecules is thought to initiate the onset of septic shock.[5–8] Interestingly, TREM-1 expression is upregulated in patients with microbial sepsis and in mice with LPS-induced septic shock.[9] Indeed, blockage of TREM-1 halted the progression of this deadly reaction and reduced mortality from 94% to 24%, for up to four hours after the outbreak of endotoxaemia.[9] TREM-1, shed from the membranes of activated phagocytes, was found in bronchoalveolar-lavage fluid of patients on ventilators, and its presence was shown to be indicative of pneumonia.[10–12] Ligation of TREM-1 triggers the differentiation of primary monocytes into immature dendritic cells and increases expression of several antigen presenting molecules. In addition, TREM-1-derived dendritic cells stimulate T cells more efficiently.[3,13] TREM-1 works synergistically with the Toll-like receptors and, although TREM-1 ligands are unknown, it is thought to recognize bacterial products, as do other pattern recognition receptors.[13]

The TREM-1 structure is of interest because (1) it is key to understanding the molecular and structural principles that determine recognition of the still elusive TREM ligands and (2) TREM-1 is a potential target for the development of septic shock therapeutics. Recently, two crystal structures of human TREM-1 were published. Radaev *et al.*[14] describe the 2.6 Å structure of a "domain-swapped dimer", whereas our laboratory, from a 1.47 Å crystal structure and a combination of crystallography and biophysical measurements, conclusively demonstrated the monomeric solution state of the soluble human and mouse TREM-1 globular ectodomain.[15] However, to provide more insight into the structure and function of TREM, and to

Abbreviations used: CDR, complementarity determining region; LPS, lipopolysaccharides.

E-mail address of the corresponding author: wilson@scripps.edu

facilitate species comparisons, we determined the crystal structure of the mouse TREM-1 (mTREM-1) immunoglobulin domain at 1.76 Å resolution.

The extracellular domain of mTREM-1, comprised of N-terminal residues 21–134, was expressed as inclusion bodies in *Escherichia coli*, refolded *in vitro* by dialysis and purified by gel-filtration and anion-exchange chromatography (see Table 1). TREM-1 crystallizes in spacegroup $P2_12_12_1$ (a=47.84 Å, b=49.08 Å and c=125.21 Å), with two monomers per asymmetric unit. The crystal structure of the receptor was determined at 1.76 Å by molecular replacement using atomic coordinates from the 1.47 Å crystal structure of human TREM-1 (hTREM-1, PDB code 1smo)[15] as a starting model. Initial $3F_o-2F_c$ electron density maps were of excellent quality and facilitated the unambiguous building of residues 25–134 of monomers A and B. After eight iterations of model building and refinement, the final model consisted of 220 protein

Table 1. Data processing and refinement statistics

A. *Data processing*	
Resolution range (outer shell) (Å)	50–1.76 (1.79–1.76)
Unique reflections	29,567 (1269)
Completeness (%)	98.3 (87.2)
Redundancy	6.3 (3.6)
R_{sym}[a] (%)	12.9 (59.5)
Average I/σ (I)	39.8 (2.5)
B. *Refinement*	
Resolution range (outer shell) (Å)	31.47–1.76 (1.81–1.76)
Reflections (test)	27,356 (1446)
R_{cryst}[b] (%)	22.5 (37.8)
R_{free}[b] (%)	24.8 (36.5)
Protein atoms	1786
Water molecules	59
Coordinate error[c] (Å)	0.11
RMSD values	
Bond lengths (Å)	0.020
Bond angles (deg.)	1.68
Dihedral angles (deg.)	6.99
$\langle B \rangle$ values (Å^2)	
Protein atoms	23.6
Water molecules	41.2
Ramachandran statistics	
Most favored (%)	88.8
Additionally allowed (%)	10.1
Generously allowed (%)	1.1

The plasmid pET-22b(+) (Novagen, Wi, USA), encoding residues 21–134 of mTREM-1, was transformed into *E. coli* BL21 (DE3) cells (Stratagene, CA, USA) and grown at 37 °C. After reaching an absorbance of 0.8 at 600 nm, recombinant expression was induced with 1 mM IPTG for three hours. Cells were harvested by centrifugation. Inclusion bodies were purified and solubilized in 8 M urea, 10 mM Tris (pH 8.0), 100 mM NaH_2PO_4, diluted to 2 mg ml^{-1} and dialyzed against 50 mM Tris (pH 8.0), 0.4 M arginine, 0.25 M NaCl, 1 mM EDTA, 1 mM GSH and 0.1 mM GSSG overnight at 4 °C. Refolded protein was then dialyzed against 10 mM Tris (pH 8.5), 5 mM 2-mercaptoethanol overnight at 4 °C and centrifuged to removed precipitated protein. Soluble, refolded protein was then purified by anion-exchange chromatography (Mono Q 10/10, Pharmacia) using a gradient (0–100%) in 10 mM Tris (pH 8.5), 5 mM 2-mercaptoethanol to 10 mM Tris (pH 8.5), 5 mM 2-mercaptoethanol, 1 M NaCl. The single, large peak containing the protein was purified to homogeneity by gel-filtration (Superdex 75 26/60, Amersham Pharmacia Biotech) into 20 mM Tris (pH 8.0), 250 mM NaCl, 1.0 mM EDTA. Typical yield was 20 mg of refolded protein from 1 l of cell culture. Crystals of mTREM-1 Ig (50 mg ml^{-1}) grew from 100 mM Mes (pH 6.0), 22% (w/v) PEG 8K, 10 mM zinc acetate, at 4 °C, after two to three weeks using the sitting-drop, vapor-diffusion method. Crystals were flash-cooled to −180 °C in cryoprotectant consisting of well buffer and 25% glycerol. A 1.76 Å data set was collected on a single crystal at beamline 11-1 at the Stanford Synchrotron Radiation Laboratory (SSRL). Data were processed and scaled with HKL2000.[24] The spacegroup is $P2_12_12_1$ with unit cell dimensions a=47.84 Å, b=49.08 Å and c=125.21 Å, and two mTREM-1 molecules per asymmetric unit (V_M=2.9 Å^3/Da) corresponding to a solvent content of 57.7%. The mTREM-1 structure was determined by molecular replacement with Phaser[25] from the CCP4[26] suite using the 1.47 Å crystal structure of hTREM-1 (PDB code 1smo[15]) as a starting model (R_{cryst}=54.1%, R_{free}=51.9%). An initial model was generated by performing a rigid body refinement (50–3.0 Å) and simulated annealing (50–1.76 Å) (R_{cryst}=45.6%, R_{free}=49.2%) using the Crystallography and NMR System software package (CNS version 1.1).[27] Initial electron density maps were of excellent quality and facilitated manual construction of the mTREM-1 structure using O.[28] Further refinement to 1.76 Å was performed in CNS.[27] The model was further rebuilt into σ_A-weighted $3F_o-2F_c$ and F_o-F_c electron density maps in O. Water molecules were assigned automatically in CNS at $>3\sigma$ F_o-F_c difference density peaks and verified by manual inspection in O. After convergence in CNS (R_{cryst}=29.8%, R_{free}=33.7%), refinement was continued with REFMAC5 using TLS refinement and with riding hydrogen atoms.[29] Care was taken to keep the R_{free} test set intact during all refinement steps. Three zinc ions from the mother liquor were included in the first round of refinement in REFMAC5. The final model (R_{cryst}=22.5%, R_{free}=24.8%; Table 1) is composed of 59 water molecules, three zinc ions and all residues in monomers A and B, except residues 21–24, which showed no interpretable electron density. The quality of the model was analyzed using the programs MolProbity,[30] WHAT IF[31] and PROCHECK.[16] All surface area calculations used the program SC[20] from the CCP4 suite with a probe radius of 1.7 Å and a dot density of 25.

[a] $R_{sym} = \sum_h \sum_i |I_i(h) - \langle I(h) \rangle| / \sum_h I(h)$, where $I_i(h)$ is the ith measurement of the h reflection and $\langle I(h) \rangle$ is the average value of the reflection intensity.

[b] $R_{cryst} = \Sigma||F_o| - |F_c||/\Sigma|F_o|$, where F_o and F_c are the structure factor amplitudes from the data and the model, respectively. R_{free} is R_{cryst} with 5% test set of structure factors.

[c] Based on maximum likelihood.

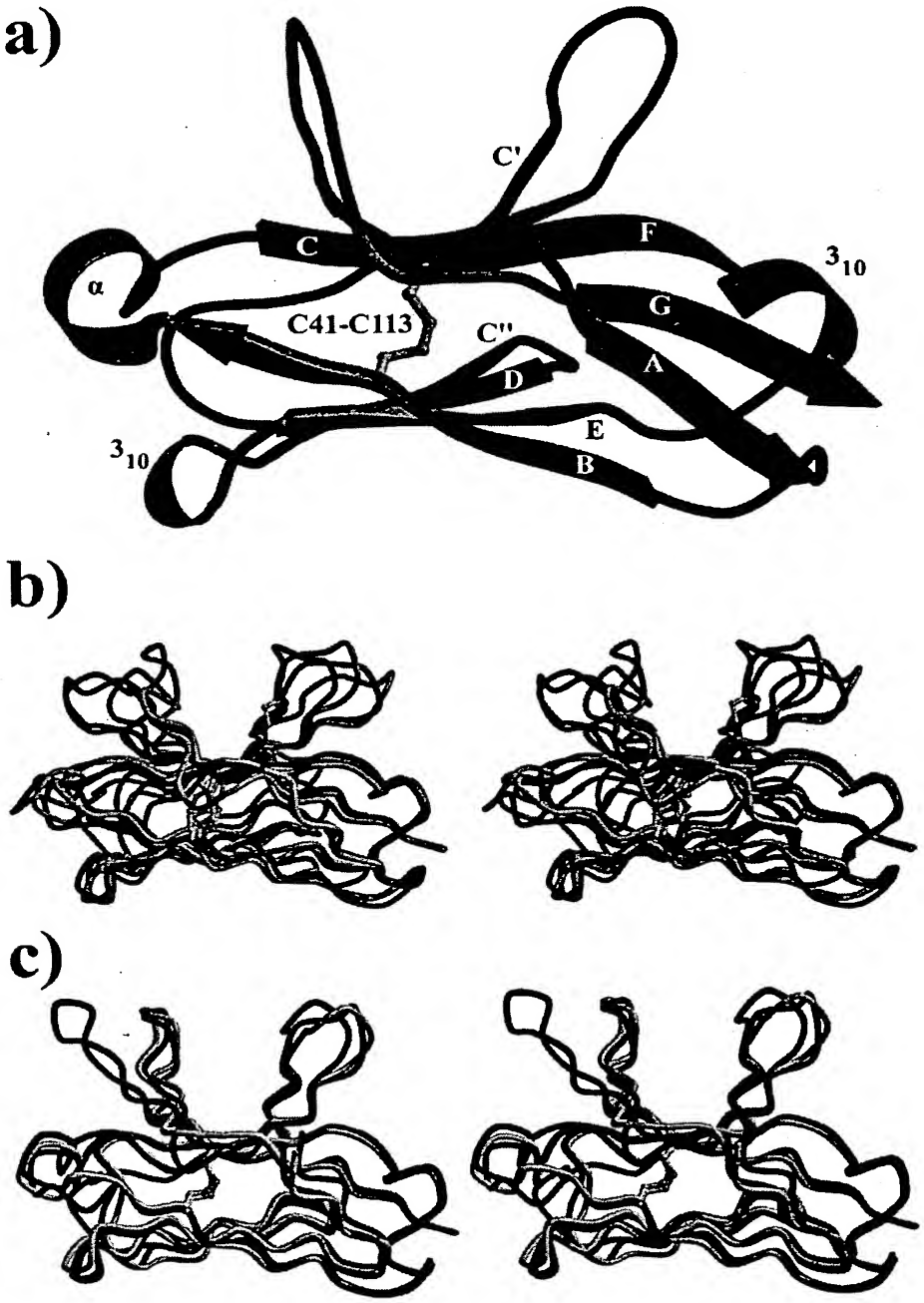

Figure 1. Stereoview of an overlay of mTREM-1 and comparison with other related immunoglobulin folds. (a) A ribbon diagram of the mTREM-1 structure determined here. (b) The mTREM-1 structure (cyan) has the expected V-set Ig domain fold seen in immunoglobulins (light blue, PDB code 1mfa), T-cell receptors (green, PDB code 1tcr) and the human natural killer cell activating receptor, NKp44 (red, PDB code 1hkf). The groove formed by β-hairpins formed by strands C–C′ and F–G is more pronounced than those in IgG, TCR or activating receptor Ig domains. Furthermore, mTREM-1 lacks the disulfide bridge (C37–C45) present only in NKp44. (c) Stereoview of a C^{α} trace of the previously published hTREM-1 structures from our laboratory (blue, 1smo),[15] Radeav *et al.*[14] (1q8m, green), and our mTREM-1 structure (red). The orientation mTREM-1 overlays in b) and c) are identical with that in a). Disulfides are labeled yellow (for carbon) and green (for sulfur). This Figure, and all subsequent ribbon diagrams, were made with Bobscript[22] and Raster3D.[23]

residues, three zinc ions from the mother liquor and 59 water molecules, with R_{cryst} and R_{free} values of 22.5% and 24.8%, respectively (Table 1). Superimposition of monomer A onto monomer B gave root-mean-square deviation (RMSD) values for main-chain atoms and for all atoms of 0.23 Å and 0.41 Å, respectively, for 110 of 110 residues. The model stereochemistry is typical at this resolution (Table 1), with 88.8% of the residues in the most favored regions, 10.1% in the additionally allowed region and two residues, Phe126 (from each monomer) in the generously allowed region of the Ramachandran plot.[16]

mTREM-1 (Figure 1(a)) is composed of nine β strands that comprise two anti-parallel β-sheets in a β-sandwich, and three helices: an α-helix (α, residues 44–49) between β-strands B and C and two 3_{10} helices, one (residues 91–93) between β-strands D and E and the other (residues 104–108), between β-strands E and F. The first β-sheet is composed of β-strands A, G, F, C and C′, and the other consists of β-strands B, E, D and C″. A hydrophobic core between β-sheets is composed of residues from strands B (Leu37 and Val39), C (Trp55), C″ (Val80 and Met82), D (Phe85 and Leu87), E (Leu96 and Val98), F (Tyr111 and Ile115) and G (Ile129 and Leu131).

mTREM-1 maintains an overall structure that is homologous to other members of the Ig family (Figure 1(b) cyan), despite a low level of sequence identity with the extracellular domain of human NKp44 (31%, PDB entry 1hkf, Figure 1(b) red), a mouse TCR V_α domain (15%, PDB entry 1tcr, Figure 1(b) green) and a mouse IgG V_H domain (15%, PDB entry 1mfa, Figure 1(b) light blue). mTREM-1 lacks the extra stabilizing disulfide bond (Cys37-Cys45) present in the activating receptor NKp44. Furthermore, NKp44 contains a positively charged groove,[17,18] formed between the β-hairpins of C–C′ and G–F, and the external face of the AGFCC′ β-sheet, which is 15 Å long, 7 Å deep and 8 Å wide, and lined with four basic residues, Arg47, His88, Arg92 and Arg106. The mTREM-1 groove is 17 Å long, 11 Å deep and 7 Å wide which, like the hTREM-1 structure, is narrower and deeper than that of NKp44. The largest difference between mTREM-1 and other V-type Ig domains are the two β-hairpins C–C′ and G–F, which protrude from the Ig domain β-sandwich.

Coordinates of mTREM-1, NKp44, the TCR V_α domain and the IgG V_H domain were subjected to structural analysis using the program DALI.[19] The DALI scores revealed similar structural homology of mTREM-1 with NKp44 (15.6; PDB entry 1hkf), mouse IgG V_H (12.7; PDB entry 1mfa), mouse TCR V_α (13.8; PDB entry 1tcr), human Vδ9–Vγ2 TCR V_γ (11.6; PDB code 1hxm) and with itself as a control (25.9). The low RMSD values for the respective core regions between mTREM-1 and NKp44 (0.75 Å, 76 of 110 C^α), mouse IgG V_H (1.23 Å, 74 of 110 C^α), mouse TCR V_α (1.29 Å, 79 of 110 C^α) and human Vδ9–Vγ2 TCR V_γ (1.23 Å, 70 of 110 C^α) further confirm the close structural relationships among members of this subset of immunoglobulin superfamily members, despite disparate biological functions.

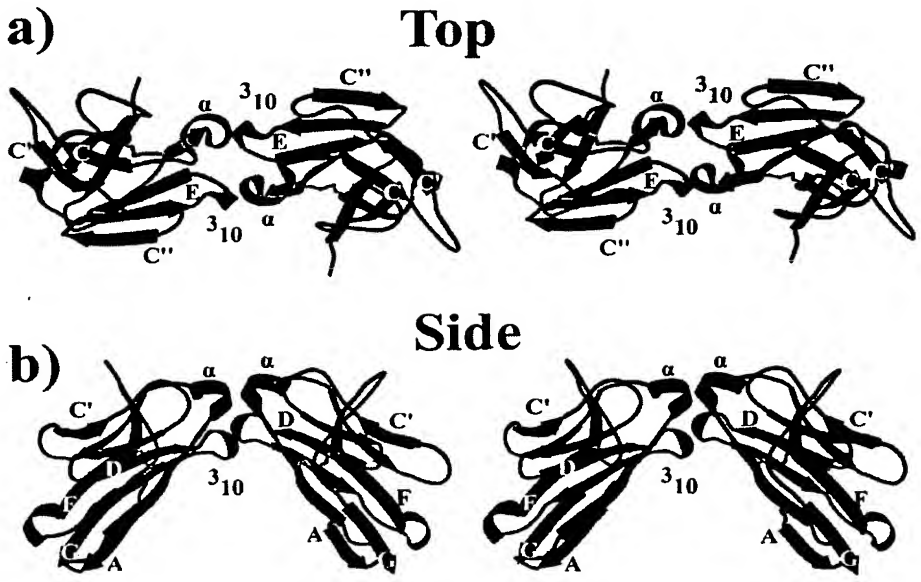

Figure 2. Contents of the mTREM-1 asymmetric unit of the crystal. The two proteins in the asymmetric unit are related by 2-fold non-crystallographic symmetry; however, given the monomeric state of the receptor,[15] this pseudo-dimeric arrangement seems to be an artifact of crystal lattice formation, consistent with its relatively small buried surface area (254 $Å^2$).

The mTREM-1 structure superimposes closely with the reported 1.47 Å hTREM-1 structure from our laboratory (PDB entry 1smo; Figure 1(c)).[15] The RMSD values for all C^{α} and main-chain atoms (110 of 110 residues) were 0.98 Å and 1.00 Å, respectively. Comparison with the 2.6 Å resolution TREM-1 structure[14] (PDB entry 1q8m) structure reveals similar three-dimensional structures. RMSD values for C^{α} and main-chain atoms (110 of 110 residues) were both 1.77 Å (Figure 1(c)). The structural differences of the F–G loop (Figure 1(c)) between our mTREM-1 structure and the previously published hTREM-1 structures suggests a region of flexibility that may be important for ligand recognition. The two mTREM-1 proteins in the asymmetric unit of the crystal form a pseudo-symmetrical dimer related by a non-crystallographic 2-fold (Figure 2). However, given the wealth of biophysical data supporting a monomeric solution state for the globular ectodomain,[15] we are confident that this symmetrical arrangement is an artifact of crystallization, and is not representative of a biologically relevant dimer. Moreover, while the calculated shape complementarity index (S_c)

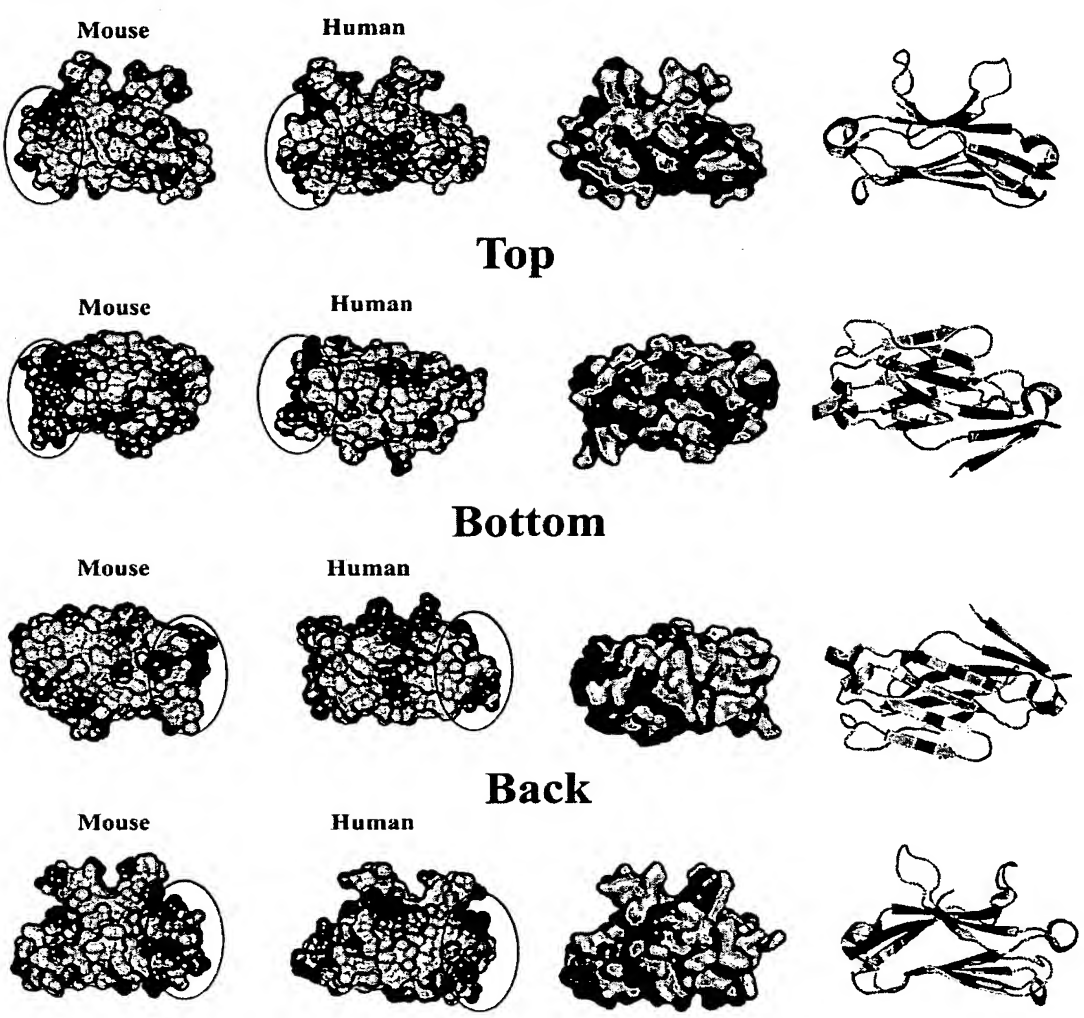

Figure 3. Electrostatic surface potential and conservation of surface residues of mTREM-1. Left: the surfaces and electrostatic potentials were generated in INSIGHTII (Molecular Simulations, Inc., San Diego, CA). Positive potential (≥10 mV) is blue, neutral potential (0 mV) is white and negative potential (−10 mV) is red. CDR-equivalent regions are marked by an oval. Right: Accessible surface area representation and ribbon diagram of the mTREM-1 Ig domain was generated using PyMOL (http://pymol.sourceforge.net/). Residues with 100% identity between the human, mouse, cow and pig TREM-1 sequences are colored green. The "Front" orientation is equivalent to that of Figure 1(a).

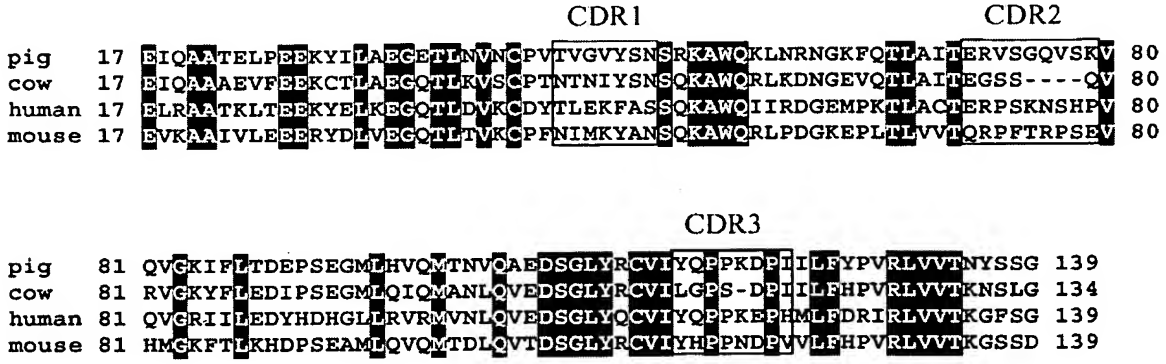

Figure 4. Sequence alignment of human, pig, mouse and cow TREM-1 extracellular immunoglobulin domains. Mouse TREM-1 was aligned with all known members of the TREM-1 family. Complete sequence conservation is labeled white within a red background. The sequences of the CDR-equivalent loops are boxed in black.

between monomer A and B was relatively good (0.69),[20] relatively little (4.5%, 254 Å^2) of the total surface area of each monomer is buried in this interface. Finally, although we have observed two monomers in the asymmetric unit of the crystal for hTREM-1,[15] our data do not eliminate other possible homo-dimeric associations upon ligand binding when TREM-1 is attached to its membrane tether.

The structural data presented here do not, unfortunately, allow for very informed speculation on precise ligand binding sites or on potential ligands; however, several interesting aspects of the structure warrant discussion. Surfaces and electrostatic potentials were calculated with INSIGHTII (Molecular Simulations, Inc., San Diego, CA) in an attempt to identify the region on mTREM-1 that might be responsible for interaction with potential ligands (Figure 3, electrostatic surfaces). mTREM-1 recognition of its cognate ligand using antibody-equivalent complementarity determining region (CDR) loops was suggested initially by Radaev *et al.*[14] The CDR-equivalent regions of mTREM-1 are almost entirely basic, unlike those of hTREM-1, which contain patches of positive and negative charges.[15] Intriguingly, TREM-2 has been shown to bind polyionic macromolecules.[21] If the CDR-equivalent regions directly, or indirectly, *via* a carrier molecule like CD14, recognize charged portions of bacterial products like LPS, then this basic region would be well suited for recognition of negatively charged groups, such as the LPS phosphate moieties. However, this role is potentially offset by the lack of conserved residues in the CDR-equivalent region (Figure 4).

Residues conserved 100% between human, pig, cow and mouse TREM-1 were mapped to the TREM-1 accessible surface area and colored green (Figure 3, right surface and ribbon diagram). While TREM-1 immunoglobulin domains are 35% identical by amino acid sequence, no large clusters of conserved residues are visible on the surface that would represent an obvious binding or interface site. The underside of the β-sandwich (Figure 3, right, bottom surface) and the CDR-equivalent regions of the TREM-1 molecules have less conservation than the corresponding top and side faces opposite the CDR-equivalent face. Interestingly, the only correlation between conserved surface accessibility and electrostatic potentials is a diagonal strip of hydrophobic residues that traverse the back of the molecule (Figure 3, back orientation).

In summary, mTREM-1 is likely a monomer in solution and superimposes closely with the previously reported hTREM-1 structures. Given the lack of conserved residues in the CDR-equivalent regions, it is unlikely that they will play a major role in direct recognition of TREM-1 ligands.

Protein Data Bank accession code

Coordinates and structure factors have been deposited in the Protein Data Bank under the accession code 1u9k.

Acknowledgements

This work was supported, in part, by NIH grants CA58896 and AI42266 to I.A.W., an NIH predoctoral training grant T32 AI077606, a Skaggs predoctoral fellowship and the Jairo H. Arévalo Fellowship to M.S.K and a Skaggs predoctoral fellowship to E.W.D. We thank Dr Xaoping Dai and Mr Thomas Bowden for data collection, and the SSRL staff of beamline 11-1 for guidance during data collection. This is manuscript number 16823-MB from The Scripps Research Institute.

References

1. Bouchon, A., Dietrich, J. & Colonna, M. (2000). Cutting edge: inflammatory responses can be

triggered by TREM-1, a novel receptor expressed on neutrophils and monocytes. *J. Immunol.* **164**, 4991–4995.
2. Daws, M. R., Lanier, L. L., Seaman, W. E. & Ryan, J. C. (2001). Cloning and characterization of a novel mouse myeloid DAP12-associated receptor family. *Eur. J. Immunol.* **31**, 783–791.
3. Bleharski, J. R., Kiessler, V., Buonsanti, C., Sieling, P. A., Stenger, S., Colonna, M. *et al.* (2003). A role for triggering receptor expressed on myeloid cells-1 in host defense during the early-induced and adaptive phases of the immune response. *J. Immunol.* **170**, 3812–3818.
4. Lanier, L. L. & Bakker, A. B. (2000). The ITAM-bearing transmembrane adaptor DAP12 in lymphoid and myeloid cell function. *Immunol. Today*, **21**, 611–614.
5. Beutler, B., Milsark, I. W. & Cerami, A. C. (1985). Passive immunization against cachectin/tumor necrosis factor protects mice from lethal effect of endotoxin. *Science*, **229**, 869–871.
6. Cohen, J. (2001). TREM-1 in sepsis. *Lancet*, **358**, 776–778.
7. Glauser, M. P., Zanetti, G., Baumgartner, J. D. & Cohen, J. (1991). Septic shock: pathogenesis. *Lancet*, **338**, 732–736.
8. Nathan, C. & Ding, A. (2001). TREM-1: a new regulator of innate immunity in sepsis syndrome. *Nature Med.* **7**, 530–532.
9. Bouchon, A., Facchetti, F., Weigand, M. A. & Colonna, M. (2001). TREM-1 amplifies inflammation and is a crucial mediator of septic shock. *Nature*, **410**, 1103–1107.
10. Gibot, S. (2004). TREM, new receptors mediating innate immunity. *Med. Sci. (Paris)*, **20**, 503–505.
11. Gibot, S., Cravoisy, A., Levy, B., Bene, M. C., Faure, G. & Bollaert, P. E. (2004). Soluble triggering receptor expressed on myeloid cells and the diagnosis of pneumonia. *N. Engl. J. Med.* **350**, 451–458.
12. Gibot, S., Kolopp-Sarda, M. N., Bene, M. C., Cravoisy, A., Levy, B., Faure, G. C. *et al.* (2004). Plasma level of a triggering receptor expressed on myeloid cells-1: its diagnostic accuracy in patients with suspected sepsis. *Ann. Intern. Med.* **141**, 9–15.
13. Colonna, M. (2003). TREMs in the immune system and beyond. *Nature Rev. Immunol.* **3**, 445–453.
14. Radaev, S., Kattah, M., Rostro, B., Colonna, M. & Sun, P. D. (2003). Crystal structure of the human myeloid cell activating receptor TREM-1. *Structure (Camb)*, **11**, 1527–1535.
15. Kelker, M. S., Foss, T. R., Peti, W., Teyton, L., Kelly, J. W., Wuthrich, K. *et al.* (2004). Crystal structure of human triggering receptor expressed on myeloid cells 1 (TREM-1) at 1.47 A. *J. Mol. Biol.* **342**, 1237–1248.
16. Laskowski, R. A., Macarthur, M. W., Moss, D. S. & Thornton, J. M. (1993). PROCHECK: a program to check the stereochemical quality of protein structures. *J. Appl. Crystallog.* **26**, 283–291.
17. Cantoni, C., Ponassi, M., Biassoni, R., Conte, R., Spallarossa, A., Moretta, A. *et al.* (2002). Crystallization and preliminary crystallographic characterization of the extracellular Ig-like domain of human natural killer cell activating receptor NKp44. *Acta Crystallog.* **58**, 1843–1845.
18. Cantoni, C., Ponassi, M., Biassoni, R., Conte, R., Spallarossa, A., Moretta, A. *et al.* (2003). The three-dimensional structure of the human NK cell receptor NKp44, a triggering partner in natural cytotoxicity. *Structure (Camb)*, **11**, 725–734.
19. Holm, L. & Sander, C. (1993). Protein structure comparison by alignment of distance matrices. *J. Mol. Biol.* **233**, 123–138.
20. Lawrence, M. C. & Colman, P. M. (1993). Shape complementarity at protein/protein interfaces. *J. Mol. Biol.* **234**, 946–950.
21. Daws, M. R., Sullam, P. M., Niemi, E. C., Chen, T. T., Tchao, N. K. & Seaman, W. E. (2003). Pattern recognition by TREM-2: binding of anionic ligands. *J. Immunol.* **171**, 594–599.
22. Esnouf, R. M. (1997). An extensively modified version of MolScript that includes greatly enhanced coloring capabilities. *J. Mol. Graph. Model.* **15**, 132–134.
23. Merritt, E. A. & Bacon, D. J. (1997). Raster3D: photorealistic molecular graphics. *Methods Enzymol.* **277**, 505–524.
24. Otwinowski, Z. & Minor, W. (1997). Processing of X-ray diffraction data collected in oscillation mode. *Methods Enzymol.* **276**, 307–326.
25. Storoni, L. C., Mccoy, A. J. & Read, R. J. (2004). Likelihood-enhanced fast rotation functions. *Acta Crystallog. sect. D*, **60**, 432–438.
26. Collaborative Computational Project, Number 4. (1994). The CCP4 suite: programs for protein crystallography. *Acta Crystallog. sect. D*, **50**, 760–763.
27. Brünger, A. T., Adams, P. D., Clore, G. M., Delano, W. L., Gros, P., Grosse-Kunstleve, R. W. *et al.* (1998). Crystallography and NMR system (CNS): a new software system for macromolecular structure determination. *Acta Crystallog. sect. D*, **54**, 905–921.
28. Jones, T. A., Zou, J. Y., Cowan, S. W. & Kjeldgaard, M. (1991). Improved methods for building protein models in electron density maps and the location of errors in these models. *Acta Crystallog. sect. A*, **47**, 110–119.
29. Winn, M. D., Isupov, M. N. & Murshudov, G. N. (2001). Use of TLS parameters to model anisotropic displacements in macromolecular refinement. *Acta Crystallog. sect. D*, **57**, 122–133.
30. Lovell, S. C., Davis, I. W., Arendall, W. B., 3rd, De Bakker, P. I., Word, J. M., Prisant, M. G. *et al.* (2003). Structure validation by Cα geometry: φ, ψ and Cβ deviation. *Proteins: Struct. Funct. Genet.* **50**, 437–450.
31. Vriend, G. (1990). WHAT IF: a molecular modeling and drug design program. *J. Mol. Graph.* **8**, 52–56.

Edited by M. Guss

(Received 16 August 2004; received in revised form 5 October 2004; accepted 5 October 2004)

doi:10.1016/j.jmb.2004.07.089 J. Mol. Biol. (2004) 342, 1237–1248

JMB

Available online at www.sciencedirect.com

SCIENCE DIRECT®

ELSEVIER

Crystal Structure of Human Triggering Receptor Expressed on Myeloid Cells 1 (TREM-1) at 1.47 Å

Matthew S. Kelker[1], Theodore R. Foss[2], Wolfgang Peti[1], Luc Teyton[3] Jeffrey W. Kelly[2], Kurt Wüthrich[1] and Ian A. Wilson[1]*

[1]*Department of Molecular Biology and The Skaggs Institute for Chemical Biology The Scripps Research Institute La Jolla, CA 92037, USA*

[2]*Department of Chemistry and The Skaggs Institute for Chemical Biology, The Scripps Research Institute, La Jolla CA 92037, USA*

[3]*Department of Immunology The Scripps Research Institute La Jolla, CA 92037, USA*

**Corresponding author*

The triggering receptor expressed on myeloid cells (TREM) family of single extracellular immunoglobulin receptors includes both activating and inhibitory isoforms whose ligands are unknown. TREM-1 activation amplifies the Toll-like receptor initiated responses to invading pathogens allowing the secretion of pro-inflammatory chemokines and cytokines. Hence, TREM-1 amplifies the inflammation induced by both bacteria and fungi, and thus represents a potential therapeutic target. We report the crystal structure of the human TREM-1 extracellular domain at 1.47 Å resolution. The overall fold places it within the V-type immunoglobulin domain family and reveals close homology with Ig domains from antibodies, T-cell receptors and other activating receptors, such as NKp44. With the additional use of analytical ultracentrifugation and ^{1}H NMR spectroscopy of both human and mouse TREM-1, we have conclusively demonstrated the monomeric state of this extracellular ectodomain in solution and, presumably, of the TREM family in general.

Keywords: crystal structure; activating receptors; TREM-1; innate immunity; immune system receptor

Introduction

During the initial stages of microbial infection, the host initiates an innate immune response to slow pathogen proliferation while the adaptive T- and B-cell responses are activated and matured. Monocyte and macrophage cells of the innate immune system lack the highly diverse repertoire of B- and T-cell receptors that define cells of the adaptive immune system. Instead, they express a variety of activating and inhibitory cell surface receptors, which have similarity in their extracellular region or ectodomains, but lack any cytoplasmic signaling domains. In order to transduce a signal, they must first associate with transmembrane adaptor proteins, such as DAP12, CD3ζ and FcRγ, which contain immunoreceptor tyrosine-based activation motifs (ITAMs). Several immunoglobulin (Ig)-like activating receptor systems have been characterized and include the paired immunoglobulin receptors,[1,2] NKp44[3] human natural killer cell receptor and the SHPS-1 family.[4] Recently, a new family of receptors expressed exclusively on myeloid cells, termed triggering receptor expressed on myeloid cells (TREMs), was described[5,6] and, as for NKp44, have only one Ig-like domain, which differentiates them from other multiple Ig-like domain activating receptors.

The various isoforms of the TREM family share low sequence identity to each other and to other members of the Ig superfamily (Figure 1). TREM-1 is expressed by neutrophils and monocytes/macrophages and is a crucial mediator of septic shock and amplification of inflammatory responses to bacteria.[5,7,8] TREM-2 is expressed by immature dendritic cells where it stimulates nitric oxide and regulates the development and function of dendritic cells, microglia and osteoclasts.[9,10] Defects in human TREM-2 expression result in Nasu-Hakola disease, a rare condition causing bone cysts and presenile dementia.[11,12] Murine TREM-3 is expressed in mouse macrophages, is upregulated in response to lipopolysaccharides and, like TREM-2, stimulates the release of nitric oxide.[13] In humans, however, TREM-3 is a pseudogene.[13]

Abbreviations used: rmsd, root-mean-square deviation; ITAMs, immunoreceptor tyrosine-based activation motifs; Ig, immunoglobulin; TREMs, triggering receptor expressed on myeloid cells; Ig-SF, Ig superfamily; ITIM, immunoreceptor tyrosine-based inhibitory motif; MAD, multi-wavelength anomalous dispersion.

E-mail address of the corresponding author: wilson@scripps.edu

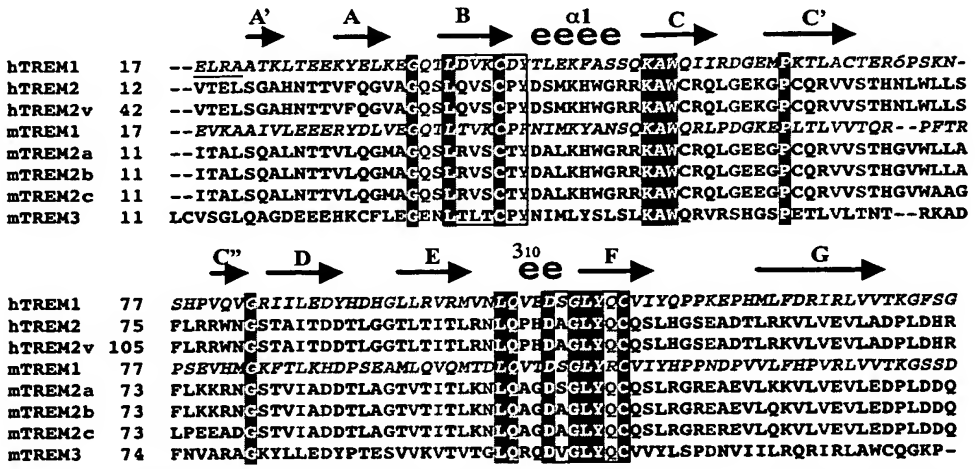

Figure 1. Sequence alignment of the extracellular immunoglobulin domains in members of the TREM family and summary of constructs used in this study. Human TREM-1 was aligned with all known members of the TREM family. Secondary structure assignments correspond to human TREM-1. Complete sequence conservation is labeled white in red background, whereas red letters correspond to > 60% sequence homology. The intrachain disulfide bridge cysteines and their flanking consensus sequences are boxed in black. Strand A′ is not visible in monomer B. Sequences for the mouse and human TREM-1 Full Ig domains are italicized. The four N-terminal residues not included in the hTREM-1 Ig domain and Ig domain + stalk constructs are underlined.

TREM-1 is an important direct link between innate and adaptive immunity.[14] Indeed, ligation of TREM-1 triggers the differentiation of primary monocytes into immature dendritic cells by stimulating the production of tumor necrosis factor-α and granulocyte/macrophage colony stimulating factor. TREM-1 also increases expression of antigen presenting molecules, CD86 and MHC Class II. Moreover, TREM-1 derived dendritic cells more efficiently present antigen to naïve T-cells and stimulate interferon-γ production by T_H1 cells.[15] Therefore, TREM-1 likely plays a role in both the adaptive and innate immune responses. Although no specific ligands have yet been identified, indirect evidence suggests that TREM-1 can recognize either bacterial products, similar to other pattern recognition receptors, or protein ligands.[15] Thus, TREMs may work synergistically with the Toll-like receptors to sense and respond to microbial infections.

Upon LPS stimulation, TREM-1 activates neutrophils and monocytes and induces the secretion of inflammatory cytokines, adhesion molecules, myeloperoxidase (neutrophils) and monocyte chemoattractant protein (MCP-1, monocytes). TREM-1 expression is upregulated in patients with microbial sepsis and mice with LPS-induced septic shock.[7] Moreover, when infected mice were treated with a TREM-1 extracellular domain—IgG F_c fusion protein, cytokine production was reduced and mortality fell from 94% to 24%. More importantly, this protection was effective up to four hours after infection.[7] Hence, TREM-1 has been implicated as a mediator of septic shock, which is caused by an excessive inflammatory reaction.[16,17] More recently, soluble TREM-1 found in bronchoalveolar-lavage fluid of patients on ventilators was demonstrated to be a clear indication of bacterial or fungal pneumonia.[18]

Human TREM-1 (hTREM-1) consists of an extracellular region of 194 amino acid residues (aa), a membrane spanning domain (29 aa) and a cytoplasmic tail (5 aa), with no signaling motifs. The extracellular Ig domain shows low sequence homology to members of the Ig superfamily (Ig-SF) and contains the motif Asp-X-Gly-X-Tyr-X-Cys, which corresponds to the signature of a V-type Ig domain.[5,19] The Ig ectodomain is connected to the transmembrane region by an ~60 residue, proline-rich linker containing three *N*-glycosylation sites, which account for the difference between the apparent molecular mass (~30 kDa) versus the predicted protein molecular mass (26 kDa).[5] The transmembrane region contains a single Lys residue which is involved in the association of TREMs with the signal transducing molecule, DAP12. The DAP12 homodimer possesses immunoreceptor tyrosine-based activation motifs (ITAMs) in its cytoplasmic domains and associates with TREM-1 via formation of a salt-bridge with an Asp residue in the transmembrane portion of DAP12.[5,20] Interestingly, the TREM gene cluster also encodes TREM-like transcripts (TLT) 1, 2 and 3, each of which contains an immunoreceptor tyrosine-based inhibitory motif (ITIM) in their cytoplasmic tails that may cause them to function as TREM inhibitors.[21,22]

The structure of TREM-1 is of particular interest for several reasons. The structure of TREM-1 is key to understanding the molecular and structural principles that determine recognition of the still elusive TREM ligands and to define the unique functions that may depend on the oligomerization

state of this activating receptor. Moreover, TREM-1 is a potential target for the development of septic shock therapeutics. Thus, we have determined the crystal structure of human TREM-1 at 1.47 Å resolution. Comparison of the TREM-1 structure to other members of the Ig-V type fold demonstrates a close structural relationship, despite very low sequence identity and disparate functions. Furthermore, this structural study, coupled with rigorous biophysical characterization of both human and mouse TREM-1, clearly demonstrates the monomeric nature of the globular ectodomain of this receptor which differs from the conclusions of a previous structural study.[23]

Results and Discussion

Structure determination

The extracellular domain of hTREM-1, comprised of N-terminal residues 21–139 (Figure 1), was expressed as inclusion bodies in *Escherichia coli*, refolded *in vitro* by dialysis and purified by gel filtration and anion exchange chromatography (see Materials and Methods). hTREM-1 crystallizes in spacegroup $P6_1$ ($a=b=110.94$ Å and $c=46.84$ Å), with two monomers per asymmetric unit. The crystal structure of the receptor was determined at 1.47 Å by the multi-wavelength anomalous dispersion (MAD) method using the anomalous signal from five selenomethionine residues. Initial $3F_o-2F_c$ electron density maps were of excellent quality and facilitated the unambiguous building of residues 21–133 of monomer A and 26–135 of monomer B. After 14 iterations of model building and refinement, the final model consisted of 223 protein residues, one tartrate molecule from the mother liquor and 175 water molecules, with R_{cryst} and R_{free} values of 19.5% and 21.2%, respectively (Table 1). Four residues, Ser^{50} and Ser^{51} of molecule A and Cys^{41} and Cys^{113} of molecule B, were found to have alternative side-chain conformations. Occupancies for each conformer were set to 0.5. Superimposition of monomer A onto monomer B gave root-mean-square deviations (rmsd's) for main-chain and all atoms of 0.81 Å and 1.18 Å, respectively. These relatively high rmsd values are due to significant

Table 1. Data processing and refinement statistics for hTREM-1 Ig domain

Data collection	SeMet			Native
Wavelength (Å)	0.9795	0.9797	0.9537	1.0000
Resolution range (Å)[a]	50–2.05 (2.12–2.05)	50–2.05 (2.12–2.05)	50–2.05 (2.12–2.05)	50–1.46 (1.49–1.46)
Unique reflections	38,108 (3792)	38,359 (3813)	37,760 (3740)	55,408 (1408)
Completeness (%)	95.5 (93.8)	96.3 (94.7)	94.7 (93.2)	96.7 (49.9)
R_{sym} (%)[b]	6.3 (17.3)	5.9 (19.8)	5.6 (26.4)	5.7 (45.2)
Average I/σ(I)	33.9 (9.1)	33.0 (7.1)	27.1 (4.1)	46.3 (3.0)
Redundancy	2.9 (2.7)	2.9 (2.7)	2.6 (2.6)	4.2 (2.9)
Overall FOM				
After SOLVE	0.40	Space group = $P6_1$		
After RESOLVE	0.66			
Refinement				
Resolution range (Å) (outer shell)	22.03–1.47 (1.51–1.47)			
Number of reflections/ test set	55,408/2,798			
R_{cryst} (%)/R_{free} (%)[c]	19.5/21.2			
Number of residues/ protein atoms	223/1,823			
Number of waters	175			
Coordinate error (Å)[d]	0.037			
rmsd from ideality				
Bonds (Å)/angles (°)/ dihedrals (°)	0.016/1.95/6.62			
Ramachandran plot				
Most favored/ additional allowed-most generously allowed/disallowed (%)	93.4/5.6/0/1.0[e]			
Average *B*-values (Å^2)				
Protein/water molecules	20.5/31.9			

[a] Numbers in parenthesis refer to the highest resolution shell.
[b] $R_{sym}=100\sum\sum|I_i(h)-\langle I(h)\rangle|/\sum I(h)$, where $I_i(h)$ is the ith measurement of the h reflection and $\langle I(h)\rangle$ is the average value of the reflection intensity.
[c] $R_{cryst}=\sum||F_o|-|F_c||/\sum|F_o|$, where F_o and F_c are the structure factor amplitudes from the data and the model, respectively. R_{free} is R_{cryst} with 5% of test set structure factors.
[d] Based on maximum likelihood.
[e] This 1.0% in disallowed regions corresponds to only one residue (Ser^{77}), but in a well-defined Type II β-turn (see the text).

deviations localized to the C–C′ and F–G loop structures and to various alternative side-chain rotamer conformations. The model stereochemistry is good (Table 1), with 93.4% of the residues in the most favored regions and one residue, Ser^{77}, in the disallowed region of the Ramachandran plot.[24] However, the electron density for Ser^{77} is excellent and locates the Ser ($\varphi = 75°$, $\psi = 140°$) to a tight type II β-turn between strands C′ and C″. Furthermore, Ser^{77} is not conserved within the TREM family, or in the human natural killer cell receptor, NKp44.

Comparison with Ig domain family members

TREM-1 (Figure 2(a) and (b), cyan) maintains an overall structure that is homologous to other members of the Ig family, despite low sequence identity with the extracellular domain of human NKp44 (27.6%, PDB entry 1hkf, Figure 2(b), red), the mouse 2C TCR V_α domain (15.6%, PDB entry 1tcr, Figure 2(b), green) and a mouse IgG V_H domain (12.9%, PDB entry 1mfa, Figure 2(b), light blue). The 3_{10} helix between E and F of TREM-1 is longer than that in the TCR V_α and comparable in size to that in human NKp44. TREM-1 lacks the extra stabilizing disulfide bond (Cys^{37}–Cys^{45}) present in the activating receptor NKp44. Furthermore, NKp44 contains a positively-charged groove,[25,26] formed between the β-hairpins of C–C′ and G–F, and the external face of the AGFCC′ β-sheet, which is 15 Å long, 7 Å deep and 8 Å wide, and lined with four basic residues, Arg^{47}, His^{88}, Arg^{92} and Arg^{106}. The largest difference between TREM-1 and other V-type Ig domains are the two β-hairpins, C–C′ and G–F which protrude from the Ig domain β-sandwich. The TREM groove is 17 Å long, 10 Å deep and 6 Å wide, which is narrower and deeper than that of NKp44. Comparison with the previously published TREM-1 at 2.6 Å resolution[23] (PDB entry 1q8m) structure reveals a similar three-dimensional structures (rmsd of all atoms and Cα atoms (110 of 110) 1.99 Å and 1.58, respectively) (Figure 3), but with significant deviations in the G–F loop which represent a potential region of plasticity.

Coordinates of TREM-1, NKp44, the TCR V_α domain and the IgG V_H domain were submitted for structural analysis using the program DALI.[27] The DALI scores revealed similar structural homology of TREM-1 with NKp44 (15.4; PDB entry 1hkf), mouse IgG V_H (12.4; PDB entry 1mfa), mouse TCR

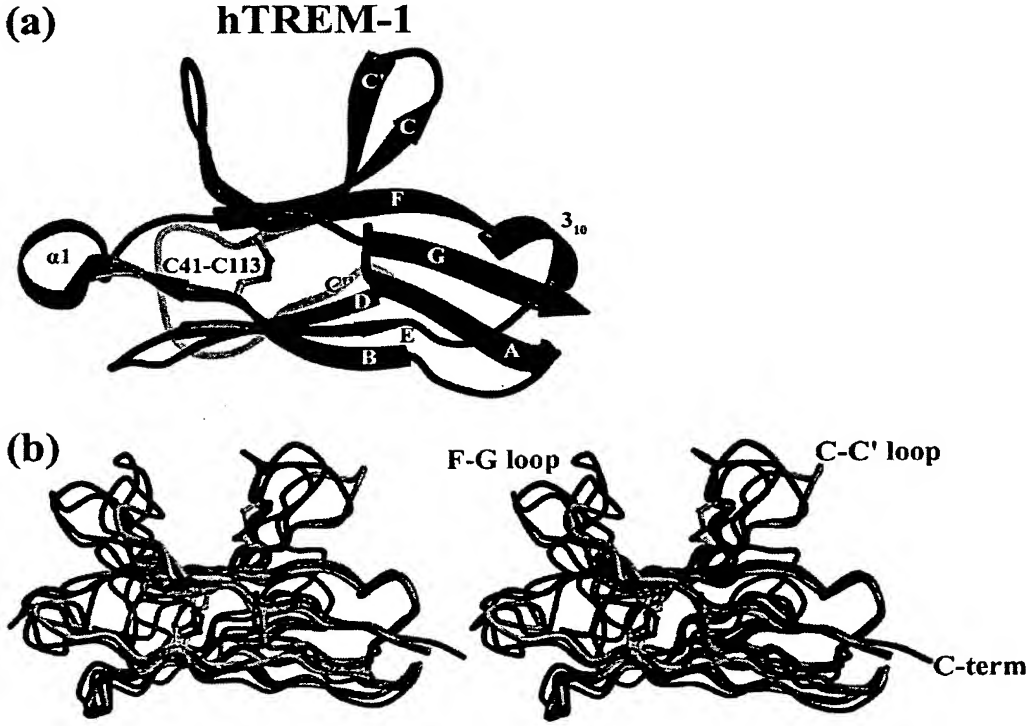

Figure 2. Stereoview of an overlay of hTREM-1 and comparison with other related immunoglobulin folds. (a) A ribbon diagram of the hTREM-1 structure determined in our study. (b) The TREM-1 structure (cyan) has the expected V-set Ig domain fold seen in immunoglobulins (light blue, PDB code 1mfa), T-cell receptors (green, PDB code 1tcr) and the human natural killer cell activating receptor, Nkp44 (red, PDB code 1hkf). The groove formed by β-hairpins formed by strands C–C′ and F–G is more pronounced than those in IgG, TCR or activating receptor Ig domains. Furthermore, hTREM-1 lacks the disulfide bridge present only in NKp44. Disulfides are labeled yellow (for carbon) and green (for sulfur). This figure and all subsequent ribbon diagram were made with Bobscript[45] and Raster3D.[46]

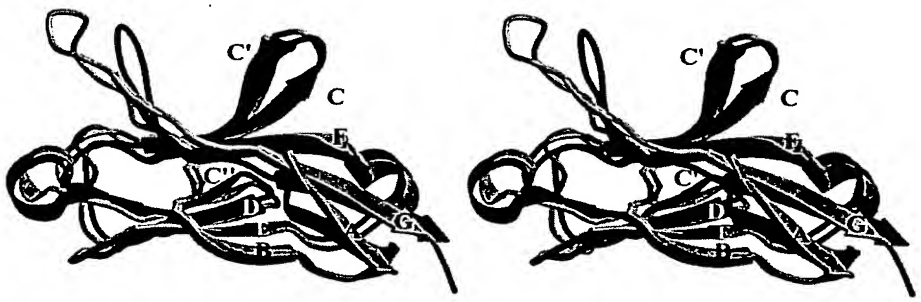

Figure 3. Stereoview of an overly of hTREM-1 from this study and the previously published TREM-1 structure. Stereoview of a C_α trace of the previously published TREM-1 structure[23] (pink) and our hTREM-1 structure (blue). Strands are labeled as in Figure 2(a).

V_α (12.9; PDB entry 1tcr), human Vδ9-Vγ2 TCR V_γ (10.8; PDB code 1hxm) and with itself as a control (25.3). The rmsd for the respective core regions (57 Cα) between TREM-1 and NKp44 (0.72 Å), mouse IgG V_H (0.98 Å) and mouse TCR V_α (0.89 Å) further confirms the close structural relationships among members of this subset of Ig-SF family members despite disparate biological functions (Figure 2).

TREM-1 ectodomain is a monomer

The web-based program Jpred[28] predicted the first several amino acid residues of the TREM-1 coding sequence to be unstructured and were, therefore, removed from our construct to increase the likelihood of success in the crystallization experiments. The two TREM-1 molecules in the asymmetric unit pack with the N and C termini oriented in the same direction (Figure 4). This interaction is asymmetric with no 2-fold NCS in which molecule A is rotated ~90° relative to B and only the first three residues (strand A) of molecule A hydrogen bond to β-strand B of molecule B. There was no interpretable electron density for the first five N-terminal residues of molecule B. Although these two monomers make extensive crystal packing contacts with other symmetry-related molecules in the crystal, none of these interactions are symmetric or suggestive of a biologically-relevant oligomer. Furthermore, while the calculated shape complementarity index (S_c) between monomer A and B was good (0.70),[29] relatively little (10%, 655 Å^2) of the total surface area of each monomer is buried in this interface.

It is possible that the unusually high protein concentrations (50–100 mg ml^{-1}) used in crystallization experiments resulted in a non-natural oligomeric state. However, during purification, TREM-1 Ig (residues 21–139, MW 13.7 kDa) existed as an 11.4 kDa monomer as observed by gel filtration (Figure 5(a), brown). The hTREM-1 Ig+ stalk (residues 21–194, MW 19.9 kDa) eluted as a ~35 kDa protein (Figure 5(a), black) but its behavior was altered, due to its helical stalk region, that permitted protein flow around matrix beads, not through them, thus reducing the retention time.

To more rigorously assess the solution state of the TREM-1 Ig domain and hTREM-1 Ig+stalk, we used sedimentation equilibrium and sedimentation velocity analytical ultracentrifugation over a broad range of protein concentrations (0.5–15 mg ml^{-1}). Sedimentation equilibrium scans of lysozyme were

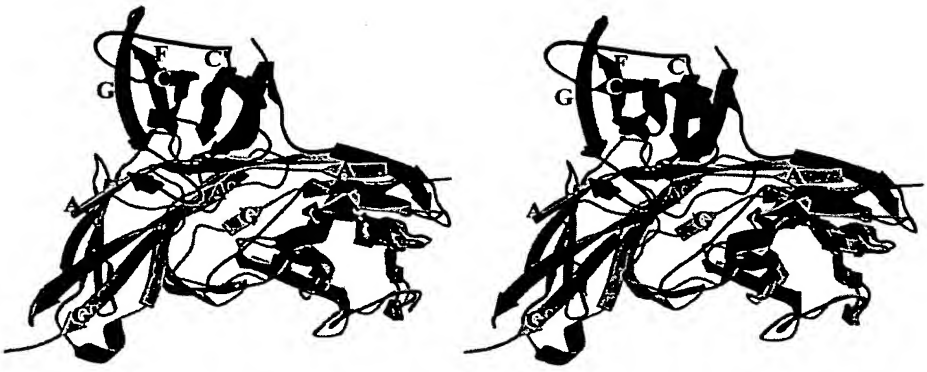

Figure 4. Stereoview of the contents of the crystal asymmetric units in this study and the previously published TREM-1 structure.[23] An overlay of the "domain-swapped dimer" (pink) and the two molecules (blue) observed in the asymmetric unit in this study. Clearly, the arrangement of the two monomers differs and is asymmetric in our study and symmetric in the "domain-swapped dimer". Strands are labeled as in Figure 2(a).

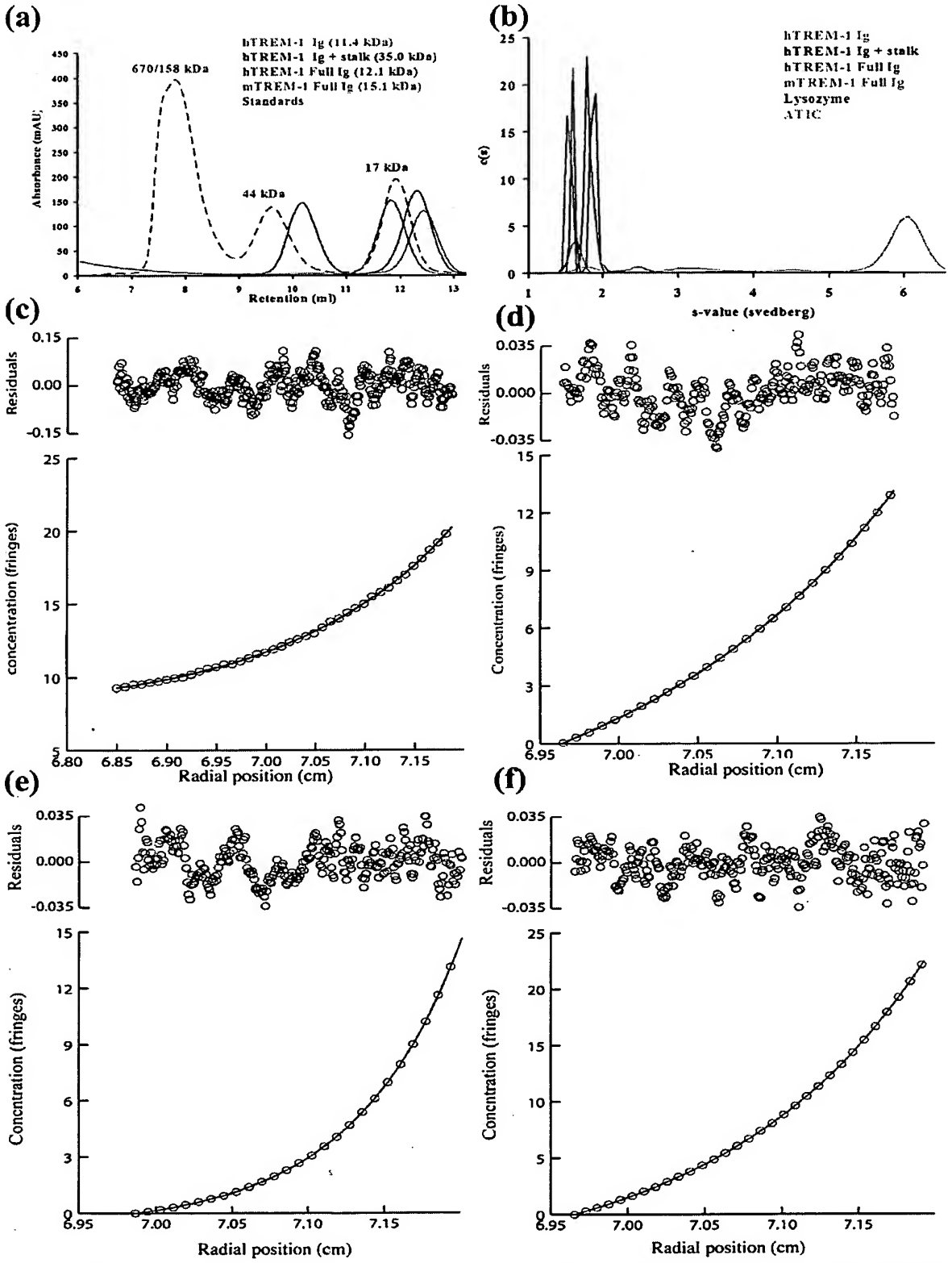

Figure 5. Biophysical studies of hTREM-1 Ig and full length proteins demonstrate monomeric nature. (a) Gel filtration

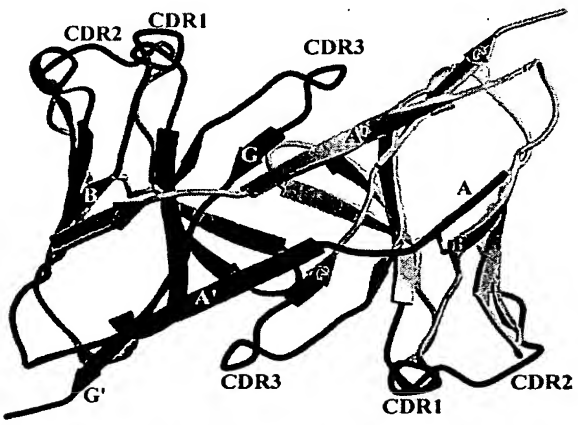

Figure 6. Ribbon diagram of the published homodimeric hTREM-1 structure. Strands A and A′ are involved in a "domain swap." The four N-terminal amino acid residues absent in our construct comprise β-strand A. Postulated binding sites that comprise the antibody equivalent complementarity determining regions (CDRs) are colored red and labeled. This figure was adapted from Figure 3 of Radaev *et al.*[23] PDB code 1q8m. Disulfides are labeled as in Figure 2.

best fit using a single species fit which yielded a molecular mass of 15,120 Da, close to the calculated mass of 14,400 Da (data not shown). Velocity data analyzed by the c(s) method[30] gave Svedberg values (Figure 5(b)) of 1.65 for the hTREM-1 Ig domain and 1.90 for the hTREM-1 Ig+stalk protein, also suggestive of monomeric states. For comparison, *S*-values of lysozyme (14,400 Da) and the bifunctional human aminoimidazole carboxamide ribonucleotide transformylase/IMP cyclohydrolase (ATIC), an ~128,000 Da dimer, were 1.8 and 6.0, respectively. The sedimentation equilibrium profiles of hTREM-1 Ig (Figure 5(c)) and hTREM-1 Ig+stalk (Figure 5(d)) proteins were best fit using single species models giving molar masses of 13,438 Da for the Ig domain and 20,206 Da, for the full length protein, in excellent agreement with their respective calculated monomer masses of 13,736 Da and 19,882 Da. Therefore, we concluded that our hTREM-1 construct is a monomer in solution.

Recently, the crystal structure of the human TREM-1 extracellular domain at 2.6 Å was published in which a "domain-swapped" homodimer was proposed (Figure 6; PDB code 1q8m).[23] The first seven amino acid residues (16–22), including the initiating methionine and the four N-terminal amino acid residues that were not present in our construct, are involved in the domain swap, such that strand A (including the initiating methionine and next four residues) of one monomer hydrogen bonds with strand B of its opposing monomer. Strand A′ then bonds to the G strand of the opposing β-sheet before continuing with the canonical hydrogen bonding to strand G′ of its own β-sheet. In our TREM-1 structure, strand A′ forms the canonical hydrogen bonds to strand G in the same domain. This TREM-1 "domain-swapped" dimer also has good surface complementarity, S_c = 0.67, but with a much more extensive buried surface area of ~1700 Å^2, corresponding to about 25% of the total monomer surface. The dimer buried surface area is still substantial (~1000 Å^2), even when the first five amino acid residues, including the initiating methionine, are removed to re-create the actual N-terminal truncation in our construct. The dimer interface is stabilized by hydrogen bonds, hydrophobic interactions and two intermolecular salt bridges between Asp^{60} to Arg^{72} and Glu^{62} to His^{123}, whereas we observed an intramolecular salt bridge between Glu^{62} and Arg^{128} in molecule B. The presence of this "domain-swapped dimer" could be partially attributed to the significantly higher crystallization salt concentrations (2.1–2.4 M ammonium sulfate), that would help mediate hydrophobic interactions in addition to fortuitous complementarity of the charged residues involved in these intermolecular salt bridges. Given the extent of the buried surface area and the extensive nature of the intermolecular interactions at the dimer interface, it was surprising that we failed to observed this dimer in our structural studies. Hence, to address the possibility that the four N-terminal amino acid residues absent from our construct were responsible for dimer formation, we used 1D ^{1}H NMR, gel filtration and analytical ultracentrifugation on both human and mouse TREM-1 full Ig domains to ascertain the oligomeric nature of these longer constructs.

To probe the solution state of the TREM-1 full Ig domains (residues 17–139) and assess the effect of pH on the oligomerization state, measurements of the transverse relaxation times (T_2) of the amide protons were carried out using a 1D ^{1}H one-one spin echo experiment[31,32] at various pH values in the range from 5.5 to 8.5. At different lengths of the echo delay (100 μs and 2.9 ms), the intensity of the amide proton signals were differently modulated so as to enable a determination of the transverse relaxation time. The intensities of 10 separated amide resonances between 8.0 and 10.4 ppm were used to extract an average T_2 relaxation time (Table 2). At pH 5.5, the average T_2 relaxation times for the human and mouse proteins were 18.0±2.4 ms and 17.0±1.6 ms, respectively. For

(Superdex 75 10/30) of hTREM-1 Ig (residues 21–139, M_r 13.7 kDa, brown), Ig+stalk (residues 21–194, M_r 19.9 kDa, black), hTREM-1 (residues 17–139, M_r 14.2 kDa, green) and mTREM-1 (residues 17–139, M_r 14.0 kDa, red) Full Ig domain proteins. Molecular weight standards are in blue. (b) Sedimentation velocity of hTREM-1 Ig, hTREM-1 Ig+stalk, hTREM-1 full Ig, mTREM-1 full Ig, lysozyme (M_r 14.4 kDa, blue) and ATIC (M_r 128 kDa, dimer, cyan). Equilibrium analytical ultracentrifugation of (c) hTREM-1 Ig, (d) hTREM-1 Ig+stalk, (e) hTREM-1 full Ig and (f) mTREM-1 full Ig.

Table 2. Values for amide proton transverse relaxation times T_2

Protein	Molecular mass (Da)	Concentration (mM (mg ml^{-1}))	pH	Average $^1H^N$ T_2 (ms)
Lysozyme	14,400	2.0 (30)	5.5	15.6±1.8
mTREM-1 full Ig	13,994	2.0 (30)		17.0±1.6
hTREM-1 full Ig	14,205	1.4 (20)		18.0±2.4
Lysozyme	14,400	2.0 (30)	6.5	16.9±3.1
mTREM-1 full Ig	13,994	2.0 (30)		17.9±2.2
hTREM-1 full Ig	14,205	0.7 (10)		18.8±2.7
Lysozyme	14,400	2.0 (30)	7.5	11.1±1.0
mTREM-1 full Ig	13,994	2.0 (30)		14.7±1.0
hTREM-1 full Ig	14,205	2.0 (30)		15.2±1.2
Lysozyme	14,400	2.0 (30)	8.5	10.9±1.4
mTREM-1 full Ig	13,994	2.0 (30)		11.9±0.9
hTREM-1 full Ig	14,205	2.0 (30)		13.6±1.6

comparison, lysozyme, which is known to be a monomer in solution with molecular weight 14,400 Da,[33–35] had an average T_2 relaxation time of 15.6±1.8 ms. Similarly at pH 6.5, human and mouse TREM-1 had average T_2 relaxation times of 18.8±2.7 ms and 17.9±2.2 ms, respectively, as compared to 16.9±3.1 ms for lysozyme. Spectra taken at pH 7.5 yielded T_2 relaxation times for human and mouse TREM-1 and lysozyme of 15.2± 1.2 ms, 14.7±1.0 ms and 11.1±1.0 ms, respectively. Finally, at pH 8.5, the average T_2 relaxation times for human and mouse TREM-1 were 13.6±1.6 ms and 11.9±0.9 ms, respectively, as compared to 10.9± 1.4 ms for lysozyme. Thus, as assessed by NMR, the TREM-1 proteins in solution are monomeric and show no pH dependent higher-order association.

As assessed by gel filtration, both human and mouse TREM-1 full Ig domains eluted at 12.1 kDa and 15.1 kDa, respectively, that approximates their expected monomeric size of ~14 kDa (Figure 5(a)). In addition, the sedimentation equilibrium scans of the human (Figure 5(e)) and mouse (Figure 5(f)) proteins were best fit using single species models giving molar masses of 13,594 Da for the human and 13,259 Da, for the mouse proteins, again, in close agreement with their respective calculated masses of 14,205 Da and 13,994 Da. Sedimentation equilibrium scans of lysozyme were also best fit using single species fits which yielded a molecular mass of 15,120 Da, close to the calculated mass of 14,400 Da (data not shown). Furthermore, sedimentation velocity experiments gave c(s) distributions with a single large peak corresponding to a Svedberg value of 1.55 for both the human and mouse TREM-1 full Ig domains, also suggestive of monomeric solution states (Figure 5(b)). The *S*-values of two control proteins, lysozyme and ATIC were 1.8 and 6.0, respectively. Moreover, although asymmetric homodimers are possible,[36] they are extremely rare in biological systems. Hence, when taken together, the biophysical and crystallographic evidence presented here, strongly suggest that in solution the globular head of the TREM-1 ectodomain is monomeric. Its oligomeric status could certainly be influenced when the intact receptor is embedded in the membrane of the cell surface or on ligand engagement, as observed for other cell membrane receptors, such as the Erythropoietin receptor.[37,38]

Biological implications

Surfaces and electrostatic potentials were calculated with INSIGHTII in an attempt to identify the region on TREM-1 that might be responsible for interaction with potential ligands; however, no such region could be identified. The predicted isoelectric point for the extracellular domain of TREM-1 is 7.15, which mirrors the overall dispersed surface electrostatic potentials, in that there is no specific localization of electrostatic charge that would suggest a potential ligand binding site (Figure 7). The structural differences of the F-G loop (Figure 3) between our hTREM-1 model and the previously published model suggests an area of flexibility which may move in response to ligation.

The unique "head-to-tail" dimer of the previously published TREM-1 structure predicts two separate ligand binding sites comprised of the equivalent CDR binding loops (Figure 6). However, given the likely monomeric state of TREM-1, and presumably of the TREM family, this bi-valent recognition mode is highly unlikely. Our data do not, however, eliminate possible homo-dimeric association upon ligand binding or of the membrane tether, as discussed above. While data presented here do not allow for more informed speculation on ligand binding sites, TREM-1 recognition of its cognate ligand using antibody-equivalent CDR loops, in an analogous fashion to TCRs, CD8 and CTLA-4, is highly feasible.

In summary, by combining crystallography and biophysical measurements, we have conclusively demonstrated the monomeric solution state of the TREM-1 globular ectodomain. Further identification of actual TREM-1 ligands and the structure of the TREM-1/ligand complex are the next crucial steps in elucidating the mechanism by which TREMs mediate the innate response to microbial products.

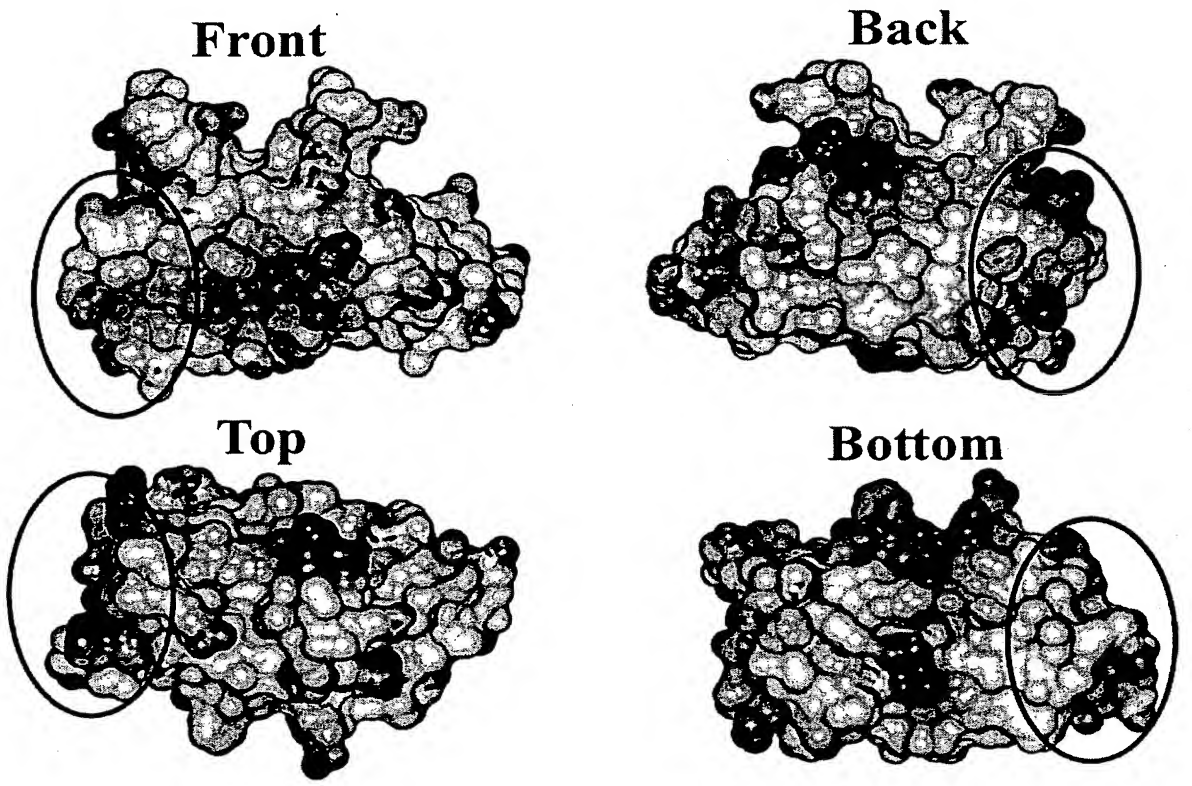

Figure 7. Electrostatic surface potential of TREM-1. The surfaces and electrostatic potentials were generated in INSIGHTII (Molecular Simulations, Inc., San Diego, CA). Positive potential (≥ 10 mV) is blue, neutral potential (0 mV) is white and negative potential ($-10 \leq$ mV) is red. CDR-equivalent regions are marked by an oval. The "Front" orientation is equivalent to that of Figures 2 and 3.

Materials and Methods

Protein expression and purification

The plasmid, pET-22b(+) (Novagen, Wi, USA) encoding residues 21–139 (Ig domain), 17–139 (full Ig domain) or 21–194 (hTREM-1 Ig+stalk) of hTREM-1 or residues 17–139 (full Ig domain) of mouse TREM-1, was transformed into *E. coli* BL21 (DE3) RIL-codon plus cells (Stratagene, CA, USA) and grown at 37 °C. After reaching an O.D. of 0.8 at 600 nm, recombinant expression was induced with 1 mM IPTG for three hours. Cells were harvested by centrifugation. Inclusion bodies were purified and solubilized in 8 M urea, 10 mM Tris pH 8.0 mM and 100 mM NaH_2PO_4, diluted to 2 mg ml^{-1} and dialyzed against 50 mM Tris, pH 8.0, 0.4 M arginine, 0.25 M NaCl, 1 mM EDTA, 1 mM GSH, 0.1 mM GSSG and 0.05% PEG 4K for 24 hours at 4 °C. Refolded protein was then dialyzed against 10 mM Tris, pH 8.5 and 5 mM 2-mercaptoethanol for 24 hours at 4 °C and centrifuged to removed precipitated protein. Soluble, refolded protein was then purified by gel filtration (Superdex 75 16/60, Amersham Pharmacia Biotech, Uppsala, Sweden) as a single peak. It was further purified by anion exchange chromatography (Mono Q 10/10, Pharmacia) using a gradient (0–100%) in 10 mM Tris, pH 8.5 and 5 mM 2-mercaptoethanol to 10 mM Tris, pH 8.5 and 5 mM 2-mercaptoethanol with 1 M NaCl. The single, large peak containing the protein was purified to homogeneity by gel filtration (Superdex 75 26/60, Amersham Pharmacia Biotech) into 20 mM Tris, pH 7.0, 100 mM NaCl, 0.5 mM EDTA and 5 mM DTT. Typical yield was 30 mg refolded protein L^{-1} cell culture. Selenomethionine-substituted protein was made by growing cells in methionine-deficient minimal medium supplemented with 50 mg L^{-1} Se-met (Sigma). Se-Met containing hTREM-1 Ig was purified as described above. Se-Met incorporation was 100% as assessed by MALDI-TOF mass spectrometry.

Crystallization and data collection

Crystals of hTREM-1 Ig (residues 21–139; 50–100 mg ml^{-1}) grew from 20% PEG 4K and 0.2 M diammonium tartrate, pH 6.3 at 4 °C, after three weeks using the sitting-drop vapor diffusion method. Crystals were 'flash-cooled' to −180 °C in cryoprotectant consisting of well buffer and 25% glycerol. A 1.47 Å native data set was collected on a single crystal at beamline 5.0.1 at the Advanced Light Source (ALS) in Berkeley (Table 1). Data for MAD phasing were collected from a second single crystal at three wavelengths (Table 1) to 2.05 Å on beamline 5.0.2 at the ALS in Berkeley. Data were processed and scaled with HKL2000.[39] The spacegroup is $P6_1$ with unit cell dimensions $a=b=110.94$ Å and $c=46.84$ Å, and two hTREM-1 molecules per asymmetric

unit (V_m=3.0 Å^3/Da) corresponding to a solvent content of 60%.

Structure determination and refinement

The positions of the selenium atoms (5 of 6) and initial phases determined by SOLVE[40] were improved by density modification using RESOLVE,[40] which resulted in the overall figure of merit (FOM) increasing from 0.40 to 0.66. The sixth selenium atom is located in a highly disordered region. These initial electron density maps were of excellent quality. The 2.05 Å maps were used for initial automated model building (8 chains, connectivity index 0.94) and refinement with ARP/wARP[41] and facilitated building of residues 21–133 of monomer A and 26–135 of monomer B using O.[42] Refinement using the native data set to 1.47 Å was performed using Crystallography and NMR System software (CNS version 1.1).[43] NCS restraints were not incorporated due to the exceptional quality and resolution of the electron density maps. The model was further rebuilt into σ_A-weighted $3F_o-2F_c$, and F_o-F_c electron density maps in O. One molecule of tartrate from the mother liquor was included in the refinement after the third round of manual rebuilding. Water molecules were assigned automatically in CNS at $>3\sigma$ F_o-F_c difference density peaks and verified by manual inspection in O. After convergence in CNS (R_{cryst}=23.1%, R_{free}=24.7%), refinement was continued with REFMAC5 using TLS refinement and with riding hydrogens.[44] Care was taken to keep the R_{free} test set intact during all refinement steps. The final model (R_{cryst}=19.3%, R_{free}=20.6%; Table 1) is composed of 175 water molecules, one tartrate molecule and all residues except residues 134–139 of monomer A and 21–25 and 136–139 of monomer B, which showed no interpretable electron density. The quality of the model was analyzed using the program PROCHECK.[24] All surface area calculations used the program SC from the CCP4 suite with a probe radius of 1.7 Å and a dot density of 25.

Coordinates

Coordinates and structure factors have been deposited in the Protein Data Bank under the accession code 1SMO.

Equilibrium analytical ultracentrifugation

The hydrodynamic molecular masses of the human and mouse TREM-1 proteins and control proteins lysozyme and human ATIC, were determined by sedimentation equilibrium measurements with a temperature-controlled Beckman XL-I Analytical Ultracentrifuge equipped with either An-60 Ti or An-50 Ti rotors using both interference and absorbance optics (Beckman Instrument Inc., Palo Alto, CA). Protein samples were loaded in a double-sector cell equipped with a 12 mm Epon centerpiece and sapphire optical windows. The proteins were dialyzed into the crystallization buffer (20 mM Tris, pH 7.0, 100 mM NaCl, 0.5 mM EDTA and 5 mM DTT) except the control protein, lysozyme, which was dialyzed against 20 mM Tris, pH 8.0, 250 mM NaCl, due to its low solubility in the TREM-1 crystallization buffer. Samples at concentrations ranging from 0.5 mg to 15 mg ml^{-1} were monitored at rotor speeds of 12,000–50,000 rpm at 20 °C and the data analyzed by a non-linear least squares approach using WinNonLin (Pharsite, Mountain View, CA) using single species and monomer-dimer models. The molar masses presented are the results of global, simultaneous fits using three rotor speeds and three or four concentrations of each protein, while the figures show a single representative fit from the set of globally fit scans. The sedimentation profiles of the human and mouse TREM-1 were best fit using single species models giving molar masses in near perfect agreement with the sequence masses. In the highest concentrations of hTREM-1 Ig (15 mg ml^{-1}), some non-specific higher order oligomerization was observed as evidenced by the higher mass of a single species fit, the inability to fit to a dimer and by non-random residuals.

Sedimentation velocity

Sedimentation velocity experiments of the human and mouse TREM-1 proteins were used for species comparisons and sedimentation coefficient determination. The proteins were dialyzed into the crystallization buffer (20 mM Tris, pH 7.0, 100 mM NaCl, 0.5 mM EDTA and 5 mM DTT) except the control proteins, lysozyme and human aminoimidazole carboxamide ribonucleotide transformylase/IMP cyclohydrolase (ATIC), which were dialyzed against 20 mM Tris, pH 8.0, 250 mM NaCl, due to low solubility in the TREM-1 crystallization buffer. The data were collected on a temperature-controlled Beckman XL-I analytical ultracentrifuge equipped with an An-60 Ti rotor and photoelectric scanner. A doublesector cell, equipped with a 12 mm Epon centerpiece and sapphire windows, was loaded with 400–420 µl of sample. Samples at concentrations ranging from 0.5 to 15 mg ml^{-1} were monitored with both absorbance and interference optics at a rotor speed of 50,000 rpm in continuous mode at 25 °C, with a step size of 0.003 cm employing an average of one scan per point. Scans were analyzed using the c(s) method from the program Sedfit, with RI and TI noise as fitted variables.[30] After initial fits, meniscus and cell bottom positions were allowed to float for the final analysis.

NMR Spectroscopy

1D ^{1}H NMR spectroscopy of the human and mouse TREM-1 full Ig domains (Figure 1) and lysozyme (Sigma, St Louis, MO; used without further purification) was used to determine the average transverse $^1H^N$ relaxation time (T_2). The unlabeled protein samples were concentrated to between 0.7 and 2.0 mM (10–30 mg ml^{-1}) and dialyzed into PBS at pH 5.5, 6.5, 7.5 or 8.5. The NMR samples consisted of 600 µl of 90% H_2O/10% D_2O containing PBS, 5 mM deuterated DTT and 0.03% mM NaN_3, except lysozyme, which contained no DTT (CIL, MA, USA). All NMR measurements were performed at 298 K on a Bruker Avance600 spectrometer equipped with five radio-frequency channels and a triple resonance probe (TXI-HCN-z gradient). The lengths of the echo delays were 100 µs and 2.9 ms. The intensities of 10 separated amide proton resonances between 8.0 and 10.4 ppm were used to extract an average T_2 relaxation time. Care was taken to compare the same $^1H^N$ lines at each pH value. The spectra were processed and analyzed using the program Xwinnmr3.5 (Bruker, Billerica, USA).

Acknowledgements

This work was supported in part by NIH grants CA58896 and AI42266 to I.A.W. and an NIH predoctorial training grant T32 AI077606, a Skaggs

predoctorial fellowship and the Jairo H. Arévalo Fellowship to M.S.K. W.P. is supported by an E. Schrödinger Fellowship by FWF (J2145) and a Max Kade Foundation Fellowship. K.W. is the Cecil H. and Ida M. Green Professor of Structural Biology. We thank Drs Xaiping Dai, Deborah Stauber and Robyn Stanfield for data collection, and the ALS staff of beamlines 5.0.1 and 5.0.2, especially Keith Henderson, for guidance during data collection. We also thank Dr James Stevens for superb technical assistance and support. This is publication 16456-MB from The Scripps Research Institute.

References

1. Kubagawa, H., Burrows, P. D. & Cooper, M. D. (1997). A novel pair of immunoglobulin-like receptors expressed by B cells and myeloid cells. *Proc. Natl Acad. Sci. USA*, **94**, 5261–5266.
2. Taylor, L. S. & McVicar, D. W. (1999). Functional association of FCε-RIγ with arginine(632) of paired immunoglobulin-like receptor (PIR)-A3 in murine macrophages. *Blood*, **94**, 1790–1796.
3. Cantoni, C., Bottino, C., Vitale, M., Pessino, A., Augugliaro, R., Malaspina, A. *et al.* (1999). NKp44, a triggering receptor involved in tumor cell lysis by activated human natural killer cells, is a novel member of the immunoglobulin superfamily. *J. Expt. Med.* **189**, 787–796.
4. Dietrich, J., Cella, M., Seiffert, M., Buhring, H. J. & Colonna, M. (2000). Cutting edge: signal-regulatory protein β1 is a DAP12-associated activating receptor expressed in myeloid cells. *J. Immunol.* **164**, 9–12.
5. Bouchon, A., Dietrich, J. & Colonna, M. (2000). Cutting edge: inflammatory responses can be triggered by TREM-1, a novel receptor expressed on neutrophils and monocytes. *J. Immunol.* **164**, 4991–4995.
6. Daws, M. R., Lanier, L. L., Seaman, W. E. & Ryan, J. C. (2001). Cloning and characterization of a novel mouse myeloid DAP12-associated receptor family. *Eur. J. Immunol.* **31**, 783–791.
7. Bouchon, A., Facchetti, F., Weigand, M. A. & Colonna, M. (2001). TREM-1 amplifies inflammation and is a crucial mediator of septic shock. *Nature*, **410**, 1103–1107.
8. Colonna, M. & Facchetti, F. (2003). TREM-1 (triggering receptor expressed on myeloid cells): a new player in acute inflammatory responses. *J. Infect. Dis.* **187**, S397–S401.
9. Bouchon, A., Hernandez-Munain, C., Cella, M. & Colonna, M. (2001). A DAP12-mediated pathway regulates expression of CC chemokine receptor 7 and maturation of human dendritic cells. *J. Expt. Med.* **194**, 1111–1122.
10. Schmid, C. D., Sautkulis, L. N., Danielson, P. E., Cooper, J., Hasel, K. W., Hilbush, B. S. *et al.* (2002). Heterogeneous expression of the triggering receptor expressed on myeloid cells-2 on adult murine microglia. *J. Neurochem.* **83**, 1309–1320.
11. Cella, M., Buonsanti, C., Strader, C., Kondo, T., Salmaggi, A. & Colonna, M. (2003). Impaired differentiation of osteoclasts in TREM-2-deficient individuals. *J. Expt. Med.* **198**, 645–651.
12. Paloneva, J., Mandelin, J., Kiialainen, A., Bohling, T., Prudlo, J., Hakola, P. *et al.* (2003). DAP12/TREM2 deficiency results in impaired osteoclast differentiation and osteoporotic features. *J. Expt. Med.* **198**, 669–675.
13. Chung, D. H., Seaman, W. E. & Daws, M. R. (2002). Characterization of TREM-3, an activating receptor on mouse macrophages: definition of a family of single Ig domain receptors on mouse chromosome 17. *Eur. J. Immunol.* **32**, 59–66.
14. Bleharski, J. R., Kiessler, V., Buonsanti, C., Sieling, P. A., Stenger, S., Colonna, M. & Modlin, R. L. (2003). A role for triggering receptor expressed on myeloid cells-1 in host defense during the early-induced and adaptive phases of the immune response. *J. Immunol.* **170**, 3812–3818.
15. Colonna, M. (2003). TREMs in the immune system and beyond. *Nature Rev. Immunol.* **3**, 445–453.
16. Cohen, J. (2001). TREM-1 in sepsis. *Lancet*, **358**, 776–778.
17. Nathan, C. & Ding, A. (2001). TREM-1: a new regulator of innate immunity in sepsis syndrome. *Nature Med.* **7**, 530–532.
18. Gibot, S., Cravoisy, A., Levy, B., Bene, M. C., Faure, G. & Bollaert, P. E. (2004). Soluble triggering receptor expressed on myeloid cells and the diagnosis of pneumonia. *N. Engl. J. Med.* **350**, 451–458.
19. Bork, P., Holm, L. & Sander, C. (1994). The immunoglobulin fold. Structural classification, sequence patterns and common core. *J. Mol. Biol.* **242**, 309–320.
20. Lanier, L. L. & Bakker, A. B. (2000). The ITAM-bearing transmembrane adaptor DAP12 in lymphoid and myeloid cell function. *Immunol. Today*, **21**, 611–614.
21. Allcock, R. J., Barrow, A. D., Forbes, S., Beck, S. & Trowsdale, J. (2003). The human TREM gene cluster at 6p21.1 encodes both activating and inhibitory single IgV domain receptors and includes NKp44. *Eur. J. Immunol.* **33**, 567–577.
22. Washington, A. V., Quigley, L. & McVicar, D. W. (2002). Initial characterization of TREM-like transcript (TLT)-1: a putative inhibitory receptor within the TREM cluster. *Blood*, **100**, 3822–3824.
23. Radaev, S., Kattah, M., Rostro, B., Colonna, M. & Sun, P. D. (2003). Crystal structure of the human myeloid cell activating receptor TREM-1. *Structure (Camb.)*, **11**, 1527–1535.
24. Laskowski, R. A., MacArthur, M. W., Moss, D. S. & Thornton, J. M. (1993). PROCHECK: a program to check the stereochemical quality of protein structures. *J. Appl. Crystallog.* **26**, 283–291.
25. Cantoni, C., Ponassi, M., Biassoni, R., Conte, R., Spallarossa, A., Moretta, A. *et al.* (2002). Crystallization and preliminary crystallographic characterization of the extracellular Ig-like domain of human natural killer cell activating receptor NKp44. *Acta Crystallog.* **58**, 1843–1845.
26. Cantoni, C., Ponassi, M., Biassoni, R., Conte, R., Spallarossa, A., Moretta, A. *et al.* (2003). The three-dimensional structure of the human NK cell receptor NKp44, a triggering partner in natural cytotoxicity. *Structure (Camb.)*, **11**, 725–734.
27. Holm, L. & Sander, C. (1993). Protein structure comparison by alignment of distance matrices. *J. Mol. Biol.* **233**, 123–138.
28. Cuff, J. A., Clamp, M. E., Siddiqui, A. S., Finlay, M. & Barton, G. J. (1998). JPred: a consensus secondary structure prediction server. *Bioinformatics*, **14**, 892–893.
29. Lawrence, M. C. & Colman, P. M. (1993). Shape complementarity at protein/protein interfaces. *J. Mol. Biol.* **234**, 946–950.

30. Schuck, P. (2000). Size-distribution analysis of macromolecules by sedimentation velocity ultracentrifugation and Lamm equation modeling. *Biophys. J.* **78**, 1606–1619.
31. Anglister, J., Grzesiek, S., Ren, H., Klee, C. B. & Bax, A. (1993). Isotope-edited multidimensional NMR of calcineurin B in the presence of the non-deuterated detergent CHAPS. *J. Biomol. NMR*, **3**, 121–126.
32. Sklenar, V. & Bax, A. (1987). Spin echo water suppression for the generation of pure phase two-dimensional NMR spectra. *J. Magn. Reson.* **74**, 469–479.
33. Redfield, C. & Dobson, C. M. (1988). Sequential ^{1}H NMR assignments and secondary structure of hen egg white lysozyme in solution. *Biochemistry*, **27**, 122–136.
34. Schwalbe, H., Grimshaw, S. B., Spencer, A., Buck, M., Boyd, J., Dobson, C. M. *et al.* (2001). A refined solution structure of hen lysozyme determined using residual dipolar coupling data. *Protein Sci.* **10**, 677–688.
35. Smith, L. J., Sutcliffe, M. J., Redfield, C. & Dobson, C. M. (1993). Structure of hen lysozyme in solution. *J. Mol. Biol.* **229**, 930–944.
36. Jin, L., Sliz, P., Chen, L., Macian, F., Rao, A., Hogan, P. G. & Harrison, S. C. (2003). An asymmetric NFAT1 dimer on a pseudo-palindromic kappa B-like DNA site. *Nature Struct. Biol.* **10**, 807–811.
37. Livnah, O., Stura, E. A., Johnson, D. L., Middleton, S. A., Mulcahy, L. S., Wrighton, N. C., Dower, W. J., Jolliffe, L. K. & Wilson, I. A. (1996). Functional mimicry of a protein hormone by a peptide agonist: the EPO receptor complex at 2.8 Å. *Science*, **273**, 464–471.
38. Livnah, O., Stura, E. A., Middleton, S. A., Johnson, D. L., Jolliffe, L. K. & Wilson, I. A. (1999). Crystallographic evidence for preformed dimers of erythropoietin receptor before ligand activation. *Science*, **283**, 987–990.
39. Otwinowski, Z. & Minor, W. (1997). Processing of X-ray diffraction data collected in oscillation mode. *Methods Enzymol.* **276**, 307–326.
40. Terwilliger, T. C. & Berendzen, J. (1996). Correlated phasing in multiple isomorphous replacement data. *Acta Crystallog. sect. D*, **52**, 749–757.
41. Lamzin, V. S. & Wilson, K. S. (1993). Automated refinement of protein models. *Acta Crystallog. sect. D*, **49**, 129–149.
42. Jones, T. A., Zou, J. Y., Cowan, S. W. & Kjeldgaard, M. (1991). Improved methods for building protein models in electron density maps and the location of errors in these models. *Acta Crystallog. sect. A*, **47**, 110–119.
43. Brünger, A. T., Adams, P. D., Clore, G. M., DeLano, W. L., Gros, P., Grosse-Kunstleve, R. W. *et al.* (1998). Crystallography and NMR system (CNS): a new software system for macromolecular structure determination. *Acta Crystallog. sect. D*, **54**, 905–921.
44. Winn, M. D., Isupov, M. N. & Murshudov, G. N. (2001). Use of TLS parameters to model anisotropic displacements in macromolecular refinement. *Acta Crystallog. sect. D*, **57**, 122–133.
45. Esnouf, R. M. (1997). An extensively modified version of MolScript that includes greatly enhanced coloring capabilities. *J. Mol. Graph. Model.* **15**, 132–134 see also 112–133.
46. Merritt, E. A. & Bacon, D. J. (1997). Raster3D: photorealistic molecular graphics. *Methods Enzymol.* **277**, 505–524.

Edited by R. Huber

(Received 24 May 2004; received in revised form 13 July 2004; accepted 26 July 2004)

A Soluble Form of the Triggering Receptor Expressed on Myeloid Cells-1 Modulates the Inflammatory Response in Murine Sepsis

Sébastien Gibot,[1,2] Marie-Nathalie Kolopp-Sarda,[3] Marie-C. Béné,[3] Pierre-Edouard Bollaert,[1] Alain Lozniewski,[4] Françoise Mory,[4] Bruno Levy,[1,2] and Gilbert C. Faure[3]

[1]*Réanimation Médicale, Hôpital Central, 54035 Nancy Cedex, France*
[2]*Laboratoire de Physiologie Expérimentale, Faculté de Médecine, 54035 Nancy Cedex, France*
[3]*Laboratoire d'Immunologie, Faculté de Médecine, 54035 Nancy Cedex, France*
[4]*Laboratoire de Bactériologie, Hôpital Central, 54035 Nancy Cedex, France*

Abstract

The triggering receptor expressed on myeloid cells (TREM)-1 is a recently discovered receptor expressed on the surface of neutrophils and a subset of monocytes. Engagement of TREM-1 has been reported to trigger the synthesis of proinflammatory cytokines in the presence of microbial products. Previously, we have identified a soluble form of TREM-1 (sTREM-1) and observed significant levels in serum samples from septic shock patients but not controls. Here, we investigated its putative role in the modulation of inflammation during sepsis. We observed that sTREM-1 was secreted by monocytes activated in vitro by LPS and in the serum of animals involved in an experimental model of septic shock. Both in vitro and in vivo, a synthetic peptide mimicking a short highly conserved domain of sTREM-1 appeared to attenuate cytokine production by human monocytes and protect septic animals from hyper-responsiveness and death. This peptide seemed to be efficient not only in preventing but also in down-modulating the deleterious effects of proinflammatory cytokines. These data suggest that in vivo modulation of TREM-1 by sTREM peptide might be a suitable therapeutic tool for the treatment of sepsis.

Key words: triggering receptor expressed on myeloid cells-1 • inflammation • sepsis • proinflammatory cytokines • mouse model

Introduction

After an infection, innate and cognitive immune responses develop in sequential phases that build up in specificity and complexity, resulting ultimately in the clearance of infectious agents and restoration of homeostasis. The innate immune response serves as the first line of defense and is initiated upon activation of pattern recognition receptors, such as Toll-like receptors (TLRs) (1, 2), by various pathogen-associated microbial patterns (3). Activation of the TLRs triggers the release of large quantities of such cytokines as TNF-α and IL-1β, which, in case of such massive infections as sepsis, can precipitate tissue injury and lethal shock (4, 5). Although antagonists of TNF-α and IL-1β appeared in this context as possibly interesting therapeutic agents of sepsis, they have unfortunately shown limited efficacy in clinical trials (6–8). This could be due to the fact that these cytokines are necessary for the clearance of infections and that their removal would allow for fatal bacterial growth (9–11).

The triggering receptor expressed on myeloid cells (TREM)-1 is a recently discovered cell-surface molecule that has been identified both on human and murine polymorphonuclear neutrophils and mature monocytes (12). It belongs to the immunoglobulin superfamily and activates downstream signaling pathways with the help of an adaptor protein called DAP12 (12–15). Bouchon and coworkers have shown that the expression of TREM-1 was greatly up-regulated on neutrophils and monocytes in the presence

Address correspondence to Sébastien Gibot, Hôpital Central, Service de Réanimation Médicale, 29 avenue du Maréchal de Lattre de Tassigny, 54035 Nancy Cedex, France. Phone: 33-3-83-85-29-70; Fax: 33-3-83-85-85-11; email: s.gibot@chu-nancy.fr

Abbreviations used in this paper: CLP, cecal ligation and puncture; TREM, triggering receptor expressed on myeloid cells; TREM-1sv, TREM-1 splice variant; TLR, toll-like receptor.

 J. Exp. Med. © The Rockefeller University Press • 0022-1007/2004/12/1419/8 $8.00
Volume 200, Number 11, December 6, 2004 1419–1426
http://www.jem.org/cgi/doi/10.1084/jem.20040708

of such bacteria as *Pseudomonas aeruginosa* or *Staphylococcus aureus*, both in cell culture and in tissue samples from patients with infection (16). In striking contrast, TREM-1 was not up-regulated in samples from patients with noninfectious inflammatory diseases such as psoriasis, ulcerative colitis, or vasculitis caused by immune complexes (16). Moreover, when TREM-1 is bound to its ligand there is a synergistic effect of LPS and an amplified synthesis of the proinflammatory cytokines TNF-α and GM-CSF, together with an inhibition of IL-10 production (17). In a murine model of LPS-induced septic shock, blockade of TREM-1 signaling protected the animals from death, further highlighting the crucial role of this molecule (13, 16).

Here we show that a soluble form of TREM-1 (sTREM-1) is released in the peripheral blood during infectious aggression in mouse. We also confirm monocytes as a major source of sTREM and show that a synthetic peptide mimicking a part of the extracellular domain of TREM-1 can modulate cytokine production by activated monocytes in vitro. We further demonstrate that the same peptide also modulates in vivo the proinflammatory cascade triggered by infection, thus inhibiting hyper-responsiveness and death in an animal model of sepsis.

Materials and Methods

Preparation of Monocytes from Peripheral Blood. 10 ml of peripheral blood samples were collected on EDTA-K from five healthy volunteer donors originating from laboratory staff. After dilution in RPMI (Life Technologies) vol/vol, blood was centrifuged for 30 min at room temperature over a Ficoll gradient (Amersham Biosciences) to isolate PBMCs. The cells recovered above the gradient were washed and counted. To deplete the suspensions of lymphocytes, cells were then plated in 24-well flat-bottom tissue culture plates (Corning) at a concentration of 5×10^6/ml and allowed to adhere during 2 h at 37°C. The resulting lymphocyte suspension was discarded, and the adhering monocytic cells were maintained in a 5% CO_2 incubator at 37°C in complete medium (RPMI 1640, 0.1 mM sodium pyruvate, 2 mM penicillin, 50 μg/ml streptomycin; Life Technologies) supplemented with 10% FCS (Invitrogen).

TREM-1 Peptide. Based on the TREM-1 sequence in GenBank/EMBL/DDBJ (under accession nos. AF287008 and AF241219), a domain highly conserved in mouse and man was found in the extracellular portion of the protein. The corresponding conserved domain (LQVTDSGLYRCVIYHPP) was chemically synthesized as a COOH terminally amidated peptide (Pepscan Systems). The correct peptide was obtained in >99% yield and with measured mass of 1,961 D versus a calculated mass of 1,962 D and was homogeneous after preparative purification, as confirmed by mass spectrometry and analytic reversed phase-high performance liquid chromatography. This peptide was called LP17. A peptide containing the same amino acids as LP17 but in a different sequence order (TDSRCVIGLYHPPLQVY) was similarly synthesized and served as control peptide.

In Vitro Stimulation of Monocytes. For activation, monocytes were cultured in the presence of *Escherichia coli* LPS (O111:B4, 1 μg/ml; Sigma-Aldrich). Cell viability was assessed by trypan blue exclusion and by measuring lactate dehydrogenase release. In some experiments, this stimulus was given in combination with TNF-α (5–100 ng/ml; R&D Systems), IL-1β (5–100 ng/ml; R&D Systems), rIFN-γ (up to 100 U/ml; R&D Systems), rIL-10 (500 U/ml; R&D Systems), or up to 100 ng/ml of LP17 or control peptide.

To activate monocytes through TREM-1, an anti–TREM-1 agonist monoclonal antibody (R&D Systems) was added as follows. Flat-bottom plates were precoated with 10 μg/ml anti–TREM-1 per well. After thorough washing in PBS, the monocyte suspensions were added at a similar concentration as above. Some experiments were performed in the presence of protease inhibitors (PMSF and Protease Cocktail Inhibitor; Invitrogen). Cell-free supernatants were assayed for the production of TNF-α and IL-1β by ELISA according to the recommendations of the manufacturer (BD Biosciences). To address the effect of LP17 on NF-κB activity in monocytes, an ELISA-based assay was performed (BD Mercury Transfactor kit; BD Biosciences). Monocytes were cultured for 24 h in the presence of *E. coli* LPS (O111:B4, 1 μg/ml), and/or an agonist anti–TREM-1 monoclonal antibody (10 μg/ml), and/or LP17 (100 ng/ml). Whole cell extracts were then prepared, and levels of NF-κB p50 and p65 were determined according to the recommendations of the manufacturer. All experiments were performed in triplicate, and data are expressed as means (SEM).

Identification and Quantitation of sTREM-1 Release. Primary monocytes suspensions were cultured as described above. The cells were treated with *E. coli* LPS (O111:B4, 1 μg/ml) for 24 h at 37°C. Cell-conditioned medium was submitted to Western blotting using an anti–TREM-1 monoclonal antibody (R&D Systems) in order to confirm the presence of 27 kD material recognized by anti–TREM-1. Soluble TREM-1 levels were measured by assessing the optical intensity of bands on immunodots by means of a reflectance scanner and the Quantity One Quantitation Software (Bio-Rad Laboratories, Inc.) as reported elsewhere (18). Soluble TREM-1 concentration from each sample was determined by comparing the optical densities of the samples with reference to standard curves generated with purified TREM-1. All measurements were performed in triplicate. The sensitivity of this technique allows the detection of sTREM-1 levels as low as 5 pg/ml.

TREM-1 RT-PCR. Total mRNA was extracted from primary monocytes cultured in the presence of LPS using a TRIzol reagent (Invitrogen) and reverse transcribed using Superscript RT II (Invitrogen) to generate cDNA. RT-PCR conditions then used for all reactions were 94°C, 30 s/65°C, 30 s/68°C, and 1 min for 30 cycles. Amplification was performed with 2.5 mM $MgCl_2$, 0.2 mM dNTP, 2.0 U *Taq* polymerase, and 20 pM 5′ and 3′ oligonucleotide primers (Proligos). The sequences of the 5′ and 3′ primer pairs used were the following: TTGTCTCAGAACTCCGAGCTGC and GAGACATCGGCAGTTGACTTGG for TREM-1 (17); GGACGGAGAGATGCCCAAGACC and ACCAGCCAGGAGAATGACAATG for TREM-1 splice variant (TREM-1sv) (19); and GGACGACATGGAGAAGATCTGG and ATAGTAATGTCACGCACGATTTCC for β-actin used as housekeeping amplicon. PCR products were run on agarose gels and visualized by ethidium bromide staining.

LPS-induced Endotoxinemia in Mice. After approval by the local ethical committee, male Balb/c mice (20–23 g) were randomly grouped and treated with *E. coli* LPS i.p. in combination with LP17 (in 500 μl normal saline) or control vector before or after LPS challenge. In some experiments, 5 μg of an anti–TREM-1 monoclonal antibody was administered i.p. 1 h after LPS injection. The viability of mice was examined every hour, or animals were killed at regular intervals. Serum samples were collected by cardiac puncture and assayed for TNF-α and IL-1β by ELISA (BD Biosciences) and for sTREM-1 levels by immunodot.

Cecal Ligation and Puncture Polymicrobial Sepsis Model. Male Balb/c mice (7–9 wk, 20–23 g) were anesthetized by i.p. administration of ketamine and xylazine in 0.2 ml sterile pyrogen-free saline. The cecum was exposed through a 1.0-cm abdominal midline incision and subjected to a ligation of the distal half followed by two punctures with a G21 needle. A small amount of stool was expelled from the punctures to ensure patency. The cecum was replaced into the peritoneal cavity and the abdominal incision closed in two layers. After surgery, all mice were injected s.c. with 0.5 ml of physiologic saline solution for fluid resuscitation and s.c. every 12 h with 1.25 mg (i.e., 50 μg/g) of imipenem. The animals were randomly grouped and treated with normal saline (n = 14), the control peptide (n = 14, 100 μg) or LP17 (100 μg) in a single injection at H0 (n = 18), H+4 (n = 18), or H+24 (n = 18). The last group of mice (n = 18) was treated with repeated injections of LP17 (100 μg) at H+4, H+8, and H+24. All treatments were diluted into 500 μl of normal saline and administered i.p. We next sought to determine the effect of various doses of LP17. For this purpose, mice (n = 15 per group) were treated with a single injection of normal saline or 10, 20, 50, 100, or 200 of LP17 at H0 after the cecal ligation and puncture (CLP) and monitored for survival. Five additional animals per group were killed under anesthesia at 24 h after CLP for the determination of bacterial count and cytokines levels. Peritoneal lavage fluid was obtained using 2 mL RPMI 1640 (Life Technologies), and blood was collected by cardiac puncture. Concentrations of TNF-α and IL-1β in the serum were determined by ELISA (BD Biosciences). For the assessment of bacterial counts, blood and peritoneal lavage fluid were plated in serial log dilutions on tryptic soy supplemented with 5% sheep blood agar plates. After plating, tryptic soy agar plates were incubated at 37°C aerobically for 24 h and anaerobically for 48 h. Results are expressed as CFU per ml of blood and CFU per mouse for the peritoneal lavage.

Statistical Analyses. Serum sTREM-1 and cytokines levels were expressed as mean (± SD). The protection against LPS lethality by LP17 was assessed by comparison of survival curves using the Log-Rank test. All statistical analyses were completed with Statview software (Abacus Concepts) and a two-tailed $P < 0.05$ was considered significant.

Results

A Soluble Form of TREM-1 Is Released from Cultured Human Monocytes after Stimulation with E. coli LPS. To identify the potential release of sTREM-1 in vitro, we stimulated human monocytes with LPS and analyzed the conditioned culture medium by SDS–PAGE. LPS stimulation induced the appearance of a 27-kD protein in a time-dependent manner (Fig. 1 A). Western blotting analysis revealed that this protein was specifically recognized by a monoclonal antibody directed against the extracellular domain of TREM-1 (Fig. 1 A). Cell viability was unaffected at LPS concentrations that induced the presence of sTREM-1 in conditioned medium, indicating that TREM-1 release was not due to cell death. Similarly, treatment of monocytes with protease inhibitors did not affect TREM-1 release (Fig. 1 A). TREM-1 mRNA levels were increased upon LPS treatment (Fig. 1 B), whereas TREM-1sv mRNA levels remained undetectable. This suggests that TREM-1 release is likely to be linked to an increased transcription of the gene and unrelated to TREM-1sv expression.

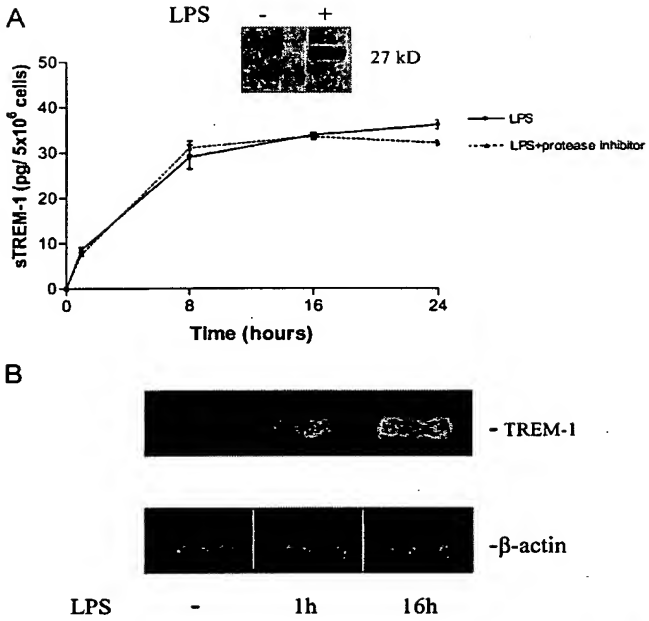

Figure 1. (A) Release of sTREM-1 from cultured monocytes after stimulation with LPS with and without proteases inhibitor. LPS stimulation induced the appearance of a 27-kD protein that was specifically recognized by an anti–TREM-1 mAb (inset). sTREM-1 levels in the conditioned culture medium were measured by reflectance of immunodots. Data are shown as mean ± SD (n = 3). (B) Expression of TREM-1 mRNA in monocytes. Cultured monocytes were stimulated with LPS (1 μg/ml) for 0, 1, and 16 h as indicated. LPS induced TREM-1 mRNA production within 1 h.

Stimulation of monocytes for 16 h with TNF-α (5–100 ng/ml) or IL-1β (5–100 ng/ml) induced very small TREM-1 release in a cytokine dose-dependent manner. Stimulation with IFN-γ did not induce TREM-1 release, even at concentrations of up to 100 U/ml.

LPS-associated Release of Proinflammatory Cytokines Is Attenuated by LP17. Significant TNF-α and IL-1β production was observed in the supernatant of monocytes cultured with LPS. TNF-α and IL-1β production was even higher for cells cultured with both TREM-1 mAb and LPS compared with those cultured with mAb or LPS alone (Fig. 2 A).

The inducible release of proinflammatory cytokines was significantly lower after LPS stimulation when the medium was supplemented with LP17 or IL-10. LP17 reduced, in a concentration-dependent manner, the TNF-α and IL-1β production from cells cultured with LPS or with LPS and mAb and simultaneously increased the release of sTREM-1 from cells cultured with LPS. The control peptide displayed no action on cytokines or sTREM-1 release (not depicted). In striking contrast, IL-10 totally inhibited the release of both TREM-1 and inflammatory cytokines (Fig. 2 A). Both LPS and TREM-1 mAb induced a strong activation of monocytic NF-κB p50 and p65, and combined administration of LPS and TREM-1 mAb lead to a synergistic effect. LP17 inhibited the NF-κB activation induced

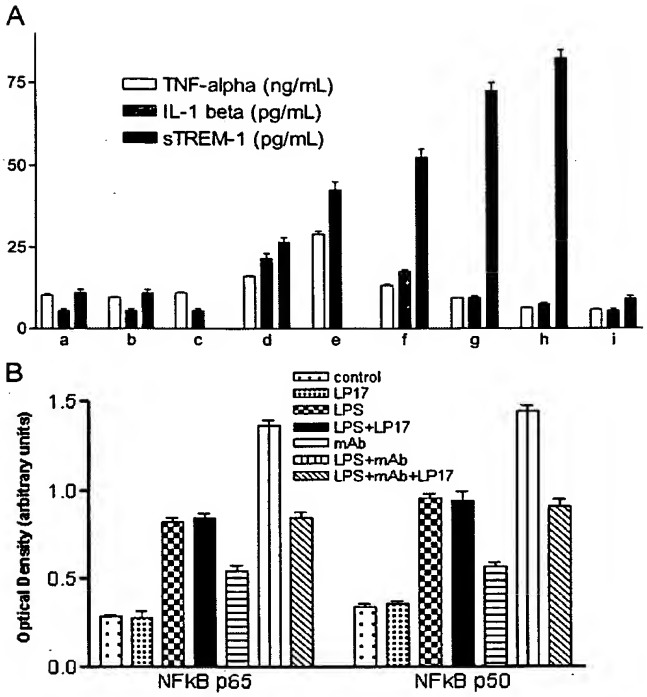

Figure 2. (A) Release of cytokines and sTREM-1 from cultured monocytes. For cell activation, primary monocytes were cultured in 24-well flat-bottom tissue culture plates in the presence of LPS (1 μg/ml). In some experiments, this stimulus was provided in combination with LP17 (10–100 ng/ml), control peptide (10–100 ng/ml), or rIL-10 (500 U/ml). To activate monocytes through TREM-1, an agonist anti–TREM-1 mAb (10 μg/ml) was added as indicated. Cell-free supernatants were analyzed for production of TNF-α, IL-1β, and sTREM-1 by ELISA or immunodot. All experiments were performed in triplicate and data are expressed as means (SEM). (a) Media; (b) LP17 10 ng/ml; (c) anti–TREM-1; (d) LPS; (e) LPS + anti–TREM-1; (f) LPS + LP17 10 ng/ml; (g) LPS + LP17 50 ng/ml; (h) LPS + LP17 100 ng/ml; (i) LPS + IL10. (B) Effect of LP17 on NF-κB activation. Monocytes were cultured for 24 h in the presence of *E. coli* LPS (O111:B4; 1 μg/ml), anti–TREM-1 mAb (10 μg/ml), and/or LP17 (100 ng/ml) as indicated, and the levels of NF-κB p50 and p65 were determined using an ELISA-based assay. Experiments were performed in triplicate, and data are expressed as means of optical densities (SEM).

by the engagement of TREM-1 but did not alter the effect of LPS (Fig. 2 B).

Serum sTREM-1 Levels of LPS-treated Mice Are Increased. To determine whether sTREM-1 was released systemically during endotoxemia in mice, we measured serum sTREM-1 levels after LPS administration. Serum sTREM-1 was readily detectable 1 h after administration of an LD_{50} dose of LPS and was maintained at peak plateau levels from 4 to 6 h after LPS treatment (Fig. 3).

LP17 Protects Endotoxemic Mice from Lethality. Mice treated by a single dose of LP17 60 min before a lethal dose (LD_{100}) of LPS were prevented from death in a dose-dependent manner (Fig. 4 A). To investigate whether LP17 treatment could be delayed until after the administration of LPS, we injected LP17 beginning 4 or 6 h after LPS injection. This delayed treatment up to 4 h conferred significant protection against an LD_{100} dose of LPS (Fig. 4 B). No late death occurred over 1 wk, indicating that LP17 did not merely delay the onset of LPS lethality but provided lasting protection. Control mice all developed lethargy, piloerection, and diarrhea before death. By contrast, LP17-

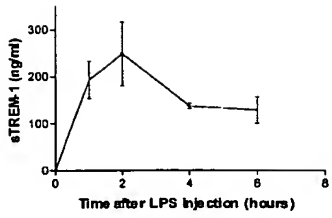

Figure 3. Accumulation of sTREM-1 in serum of LPS-treated mice. Male Balb/c mice (20–23 g) were treated with LPS (LD_{50}, intraperitoneally). Serum was assayed for sTREM-1 by immunodot. Serum sTREM-1 was readily detectable 1 h after LPS administration and was maintained at a plateau level from 4 to 6 h.

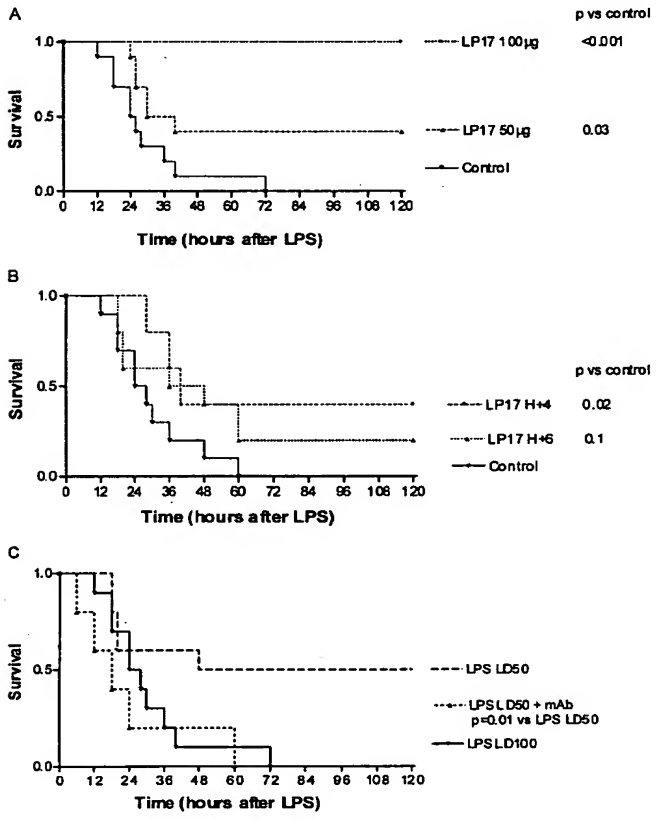

Figure 4. Endotoxinic shock in mice. (A) LP17 pretreatment protects against LPS lethality in mice. Male Balb/c mice (20–23 g) were randomly grouped (10 mice per group) and treated with an LD_{100} of LPS. LP17 (50 or 100 μg) or control vector was administered 60 min before LPS. (B) Delayed administration of LP17 protects LPS lethality in mice. Male Balb/c mice (20–23 g) were randomly grouped (8 mice per group) and treated with an LD_{100} of LPS. LP17 (75 μg) or control vector was administered 4 or 6 h after LPS as indicated. (C) Administration of agonist TREM-1 mAb is lethal to mice. Male Balb/c mice (20–23 g) were randomly grouped (eight mice per group) and treated with a combination of an LD_{50} of LPS + control vector, LD_{50} of LPS + anti-TREM-1 mAb (5 μg), or LD_{100} of LPS + control vector as indicated. Control vector and anti–TREM-1 mAb were administered 1 h after LPS injection.

Table I. *Serum Concentrations of TNF-α, IL-1β, and sTREM-1 in Endotoxemic Mice*

	TNF-α		IL-1β		sTREM-1	
	ng/mL		*ng/mL*		*ng/mL*	
	H2	H4	H2	H4	H2	H4
Control	3.3 ± 1.0	0.4 ± 0.1	0.3 ± 0.1	1.5 ± 0.2	249 ± 48	139 ± 8
LP17 (100 μg)	2.4 ± 0.5	0.1 ± 0.1	0.2 ± 0.1	0.9 ± 0.2	475 ± 37	243 ± 28

treated mice remained well groomed and active, had no diarrhea, and were lively. To clarify the mechanism by which LP17 protected mice from LPS lethality, we determined the serum levels of TNF-α, IL-1β, and sTREM-1 of endotoxemic mice at 2 and 4 h. Compared with controls, pretreatment by 100 μg of LP17 reduced cytokines levels by 30% and increased sTREM-1 levels by twofold (Table I).

Engagement of TREM-1 Is Lethal to Mice. To further highlight the role of TREM-1 engagement in LPS-mediated mortality, mice were treated with agonist anti–TREM-1 mAb in combination with the administration of an LD_{50} dose of LPS. This induced a significant increase in mortality rate from 50 to 100% (Fig. 4 C).

LP17 Protects Mice from CLP-induced Lethality. To investigate the role of LP17 in a more relevant model of septic shock, we performed CLP experiments (Fig. 5 A). The control groups comprised mice injected with normal saline or with the control peptide. In this model of polymicrobial sepsis, LP17 still conferred a significant protection against lethality even when administered as late as 24 h after the onset of sepsis. Interestingly, repeated injections of LP17 had the more favorable effect on survival ($P < 0.01$). There was a dose–response effect of LP17 on survival (Fig. 5 b) and cytokines production (Table II). LP17 had no effect on bacterial clearance (Fig. 6).

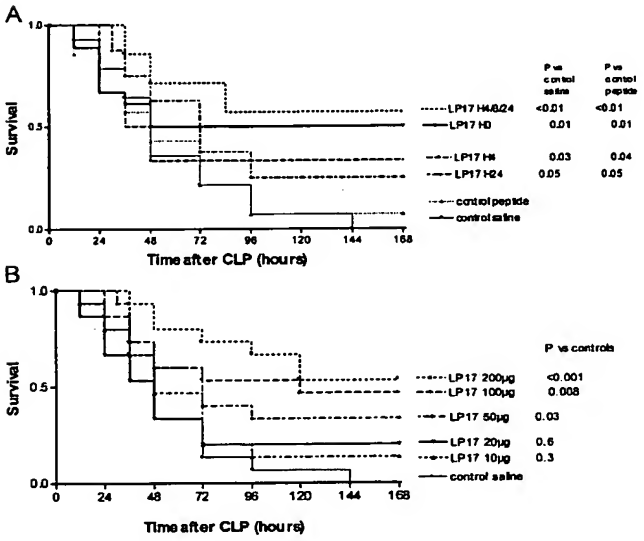

Figure 5. CLP polymicrobial sepsis model. (A) LP17 partially protects mice from CLP-induced lethality. Male Balb/c mice (20–23 g) were randomly grouped and treated with normal saline ($n = 14$) or the control peptide ($n = 14$; 100 μg) or with LP17 (100 μg) in a single infection at H0 ($n = 18$), H+4 ($n = 18$), or H+24 ($n = 18$). The last group of mice ($n = 18$) was treated with repeated injections of LP17 (100 μg) at H+4, H+8, and H+24. (B) Dose effect of LP17 on survival. Mice ($n = 15$ per group) were treated with a single injection of normal saline or 10, 20, 50, 100, or 200 μg of LP17 at H0 after the CLP and monitored for survival.

Discussion

Sepsis exemplifies a complex clinical syndrome that results from a harmful or damaging host response to severe infection. Sepsis develops when the initial, appropriate host response to systemic infection becomes amplified and then dysregulated (4, 5). Neutrophils and monocyte/macrophages exposed to LPS, for instance, are activated and release such proinflammatory cytokines as TNF-α and IL-1β. Excessive production of these cytokines is widely believed to contribute to the multiorgan failure that is seen in septic patients (20–23).

TREM-1 is a recently identified molecule involved in monocytic activation and inflammatory response (12, 14). It belongs to a family related to NK cell receptors that activate downstream signaling events. The expression of TREM-1 on PMNs and monocytes/macrophages has been shown to be inducible by LPS (16, 17).

Table II. *Serum Concentrations of TNF-α, IL-1β, and sTREM-1 at 24 h after CLP*

	TNF-α pg/mL	IL-1β pg/mL	sTREM-1 ng/mL
Control peptide	105 ± 12	841 ± 204	35 ± 5
Control saline	118 ± 8	792 ± 198	35 ± 5
LP17 10 μg	110 ± 11	356 ± 62	43 ± 8
LP17 20 μg	89 ± 10	324 ± 58	58 ± 8
LP17 50 μg	24 ± 6	57 ± 11	93 ± 10
LP17 100 μg	20 ± 3	31 ± 3	118 ± 12
LP17 200 μg	21 ± 7	37 ± 8	158 ± 13

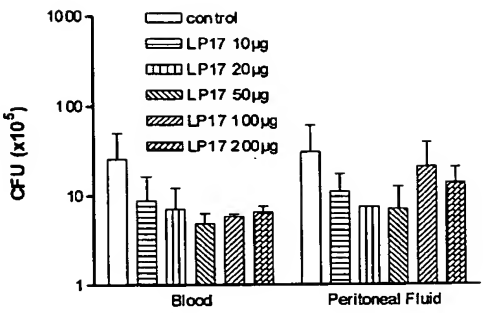

Figure 6. LP17 has no effect on bacterial counts during CLP. Mice (5 per group) were killed under anesthesia at 24 h after CLP. Bacterial counts in peritoneal lavage fluid and blood were determined and results are expressed as CFU per ml of blood and CFU per mouse for the peritoneal lavage.

Here, we report that a soluble form of TREM-1 was released from cultured human monocytes after stimulation with *E. coli* LPS. Such a soluble form was also detectable in the serum of endotoxemic mice as early as 1 h after LPS challenge. This is consistent with the implication of TREM-1 in the very early phases of the innate immune response to infection (14, 15, 24). The mechanism by which sTREM-1 is released is not clearly elucidated but seems to be related to an increased transcription of the TREM-1 gene. Nevertheless, although incubation with a protease inhibitor cocktail does not alter the sTREM-1 release, cleavage of the surface TREM-1 from the membrane cannot be totally excluded. Interestingly, stimulation of human monocytes with such proinflammatory cytokines as TNF-α, IL-1β, or IFN-γ induced very small sTREM-1 release unless LPS was added as a costimulus. The expression of an alternative mRNA TREM-1sv has been detected in monocytes that might translate into a soluble receptor (18) upon stimulation with cell wall fraction of *Mycobacterium bovis* BCG but not LPS (25). This was confirmed in this study as (a) LPS did not increase the level of mRNA TREM-1sv in monocytes and (b) only a 27-kD protein was released by monocytes upon LPS stimulation and not the 17.5-kD variant.

Although its natural ligand has not been identified (13, 14), engagement of TREM-1 on monocytes with an agonist monoclonal antibody resulted in a further enhancement of proinflammatory cytokines production, whereas LP17 induced a decrease of these syntheses in a concentration-dependent manner, and IL-10 completely suppressed it.

Inflammatory cytokines, and especially TNF-α, are considered to be deleterious, yet they also possess beneficial effects in sepsis (5) as shown by the fatal issue of peritonitis in animals with impaired TNF-α responses (9–11). Moreover, in clinical trials the inhibition of TNF-α increased mortality (8). Finally, the role of TNF-α in the clearance of infection has been highlighted by the finding that sepsis is a frequent complication in rheumatoid arthritis patients treated with TNF-α antagonists (26).

The mechanism by which LP17 modulates cytokine production is not yet clear. LP17 comprises the complementary determining region-3 and the "F" β strand of the extracellular domain of TREM-1. The latter contains a tyrosine residue mediating dimerization. Radaev et al. postulated that TREM-1 captures its ligand with its complementary determining region-equivalent loop regions (27). Thus, LP17 could impair the TREM-1 dimerization and/or compete with the natural ligand of TREM-1. Moreover, the increase of sTREM-1 release from monocytes mediated by LP17 could prevent the engagement of membrane TREM-1, sTREM-1 acting as a decoy receptor, as in the TNF-α system (28, 29).

Activation of the transcription factor NF-κB is a critical step in monocyte inflammatory cytokine production after exposure to bacterial stimuli such as LPS (30, 31). Among the various NF-κB/Rel dimers, the p65/p50 heterodimer is the prototypical form of LPS-inducible NF-κB in monocytes (32). LP17 abolishes the p65/p50 NF-κB overactivation induced by the engagement of TREM-1. This might at least partially explain the effects of LP17 on cytokine production and the protection from lethality shown here to occur when the peptide was injected 1 h before LPS-induced septic shock, or even up to 4 h after.

Endotoxemia is simple to achieve experimentally but imperfectly suited to reproduce human sepsis, whereas polymicrobial sepsis induced by CLP is a more complex but better model, including the use of fluid resuscitation and antibiotics. Thus, the latter was also used in this study and confirmed the dose-dependent protection provided by LP17, even when administered as late as 24 h after the onset of sepsis. However, the favorable effect of LP17 was unrelated to an enhanced bacterial clearance.

One difficulty in the use of immunomodulatory therapies is that it is not possible to predict the development of sepsis, and thus patients receiving those treatments frequently already have well-established sepsis (6). Since LP17 appeared to be effective even when injected after the outbreak of sepsis, it could thus constitute a realistic treatment (24, 33).

By contrast, engagement of TREM-1 by an agonist anti–TREM-1 monoclonal antibody mediated a dramatic increase of mortality rate in LPS-challenged mice: this further underscores the detrimental effect of TREM-1 engagement during septic shock.

Experimental septic shock reproduces human sepsis only in part. Indeed, our group recently showed that significant levels of sTREM-1 were released in the serum of critically ill patients with sepsis patients (34), the highest levels being observed in patients who survived. This is consistent with our experimental findings indicating that the more important sTREM-1 release, the more favorable is the outcome, and thus sustains, at least theoretically, the potential value of soluble TREM peptides as postonset sepsis therapy.

TREM-1 appears to be a crucial player in the immediate immune response triggered by infection. In the early phase of infection, neutrophils and monocytes initiate the inflammatory response owing to the engagement of pattern recognition receptors by microbial products (3, 4). At the same time, bacterial products induce the up-regulation and

the release of sTREM-1. Upon recognition of an unknown ligand, TREM-1 activates signaling pathways which amplify these inflammatory responses, notably in monocytes/macrophages. The modulation of TREM-1 signaling reduces, although without complete inhibition, cytokine production and protects septic animals from hyper-responsiveness and death. Modulation of TREM-1 engagement with such a peptide as LP17 might be a suitable therapeutic tool for the treatment of sepsis, particularly because it seems to be active even after the onset of sepsis after infectious aggression.

We are indebted to Chantal Montemont and Eliane Vauthier for technical assistance.

This work was supported in part by a grant (EA 3143) from the French Ministère de la Recherche et de la Technologie.

The authors have no conflicting financial interests.

Submitted: 9 April 2004
Accepted: 20 October 2004

References

1. Aderem, A, and R.J. Ulevitch, R.J. 2000. Toll-like receptors in the induction of the innate immune response. *Nature.* 406: 782–786.
2. Thoma-Uszynski, S., S. Stenger, O. Takeuchi, M.T. Ochoa, P.A. Engele, P.A. Sieling, P.F. Barnes, M. Rollinghoff, P.L. Bolcskei, and M. Wagner. 2001. Induction of direct antimicrobial activity through mammalian Toll-like receptors. *Science.* 291:1544–1549.
3. Medzhitov, R., and C. Janeway Jr. 2000. Innate immunity. *N. Engl. J. Med.* 343:338–344.
4. Cohen, J. 2002. The immunopathogenesis of sepsis. *Nature.* 420:885–891.
5. Hotchkiss, R.S., and I.E. Karl. 2003. The pathophysiology and treatment of sepsis. *N. Engl. J. Med.* 348:138–150.
6. Vincent, J.L., Q. Sun, and M.J. Dubois. 2002. Clinical trials of immunomodulatory therapies in severe sepsis and septic shock. *Clin. Infect. Dis.* 34:1084–1093.
7. Riedemann, N.C., R.F. Guo, and P. Ward. 2003. Novel strategies for the treatment of sepsis. *Nat. Med.* 9:517–524.
8. Fisher, C.J., Jr., J.M. Agosti, S.M. Opal, S.F. Lowry, R.A. Balk, J.C. Sadoff, E. Abraham, R.M. Schein, and E. Benjamin. 1996. Treatment of septic shock with the tumor necrosis factor receptor:Fc fusion protein. The soluble TNF receptor sepsis study group. *N. Engl. J. Med.* 334:1697–1702.
9. Echtenacher, B., W. Falk, D.N. Mannel, and P.H. Krammer. 1990. Requirement of endogenous tumor necrosis factor/cachectin for recovery from experimental peritonitis. *J. Immunol.* 145:3762–3766.
10. Echtenacher, B., K. Weigl, N. Lehn, and D.N. Mannel. 2001. Tumor necrosis factor-dependent adhesions as a major protective mechanism early in septic peritonitis in mice. *Infect. Immun.* 69:3550–3555.
11. Eskandari, M.K., G. Bolgos, C. Miller, D.T. Nguyen, L.E. DeForge, and D.G. Remick. 1992. Anti-tumor necrosis factor antibody therapy fails to prevent lethality after cecal ligation and puncture or endotoxemia. *J. Immunol.* 148:2724–2730.
12. Bouchon, A., J. Dietrich, and M. Colonna. 2000. Inflammatory responses can be triggered by TREM-1, a novel receptor expressed on neutrophils and monocytes. *J. Immunol.* 164: 4991–4995.
13. Colonna, M., and F. Facchetti. 2003. TREM-1 (triggering receptor expressed on myeloid cells): a new player in acute inflammatory responses. *J. Infect. Dis.* 187:S397–S401.
14. Colonna, M. 2003. TREMs in the immune system and beyond. *Nat. Rev. Immunol.* 3:445–453.
15. Nathan, C., and A. Ding. 2001. TREM-1: a new regulator of innate immunity in sepsis syndrome. *Nat. Med.* 7:530–532.
16. Bouchon, A., F. Facchetti, M.A. Weigand, and M. Colonna. 2001. TREM-1 amplifies inflammation and is a crucial mediator of septic shock. *Nature.* 410:1103–1107.
17. Bleharski, J.R., V. Kiessler, C. Buonsanti, P.A. Sieling, S. Stenger, M. Colonna, and R.L. Modlin. 2003. A role for triggering receptor expressed on myeloid cells-1 in host defense during the early-induced and adaptive phases of the immune response. *J. Immunol.* 170:3812–3818.
18. Gibot, S., A. Cravoisy, B. Levy, M.C. Béné, G. Faure, and P.E. Bollaert. 2004. Soluble triggering receptor expressed on myeloid cells and the diagnosis of pneumonia. *N. Engl. J. Med.* 350:451–458.
19. Gingras, M.C., H. Lapillonne, and J.F. Margolin. 2002. TREM-1, MDL-1, and DAP12 expression is associated with a mature stage of myeloid development. *Mol. Immunol.* 38: 817–824.
20. Dinarello, C.A. 1997. Proinflammatory and anti-inflammatory cytokines as mediators in the pathogenesis of septic shock. *Chest.* 112:S321–S329.
21. Bone, R.C. R.A Balk, F.B. Cerra, R.P. Dellinger, A.M. Fein, W.A. Knauss, R.M. Schein, and W.J. Sibbald. 1992. Definitions for sepsis and organ failure and guidelines for the use of innovative therapies in sepsis. The ACCP/SCCM Consensus Conference Committee. American in sepsis. The ACCP/SCCM Consensus Conference Committee. American College of Chest Physicians/Society of Critical Care Medicine. *Chest.* 101:1644–1655.
22. Warren, H.S. 1997. Strategies for the treatment of sepsis. *N. Engl. J. Med.* 336:952–953.
23. Stone, R. 1994. Search for sepsis drugs goes on despite past failures. *Science.* 264:365–367.
24. Cohen, J. 2001. TREM-1 in sepsis. *Lancet.* 358:776–778.
25. Begum, N.A., K. Ishii, M. Kurita-Taniguchi, M. Tanabe, M. Kobayashi, Y. Moriwaki, M. Matsumoto, Y. Fukumori, I. Azuma, K. Toyoshima, and T. Seya. 2004. *Mycobacterium bovis* BCG cell wall-specific differentially expressed genes identified by differential display and cDNA substraction in human macrophages. *Infect. Immun.* 72:937–948.
26. Keane, J., S. Gershon, R.P. Wise, E. Mirabile-Levens, J. Kasznica, W.D. Schwieterman, J.N. Siegel, and M.M. Braun. 2001. Tuberculosis associated with infliximab, a tumor necrosis factor alpha-neutralizing agent. *N. Engl. J. Med.* 345: 1098–1104.
27. Radaev, S., M. Kattah, B. Rostro, M. Colonna, and P. Sun. 2003. Crystal structure of the human myeloid cell activating receptor TREM-1. *Structure.* 11:1527–1535.
28. Lantz, M., U. Gullberg, and E. Nilsson. 1990. Characterization in vitro of a human tumor necrosis factor binding protein. A soluble form of tumor necrosis factor receptor. *J. Clin. Invest.* 86:1396–1401.
29. van Zee, K.J., T. Kohno, and E. Fischer. 1992. Tumor necrosis soluble receptors circulate during experimental and clinical inflammation and can protect against excessive tumor necrosis factor α in vitro and in vivo. *Proc. Natl. Acad. Sci. USA.* 89:4845–4853.

30. Collart, M.A., P. Baeuerle, and P. Vassalli. 1990. Regulation of tumor necrosis factor alpha transcription in macrophages. Involvement of four NFκB motifs and constitutive and inducible form of NFκB. *Mol. Cell. Biol.* 10:1498–1506.
31. Hiscott, J.M., J.J. Garoufalis, A. Roulston, I. Kwan, N. Pepin, J. Lacoste, H. Nguyen, G. Bensi, and M. Fenton. 1993. Characterization of a functional NFκB site in the human IL-1β promoter: evidence for a positive autoregulatory loop. *Mol. Cell. Biol.* 13:6231–6240.
32. Urban, M.B., R. Schreck, and P.A. Baeuerle. 1991. NFκB contacts DNA by a heterodimer of the p50 and p65 subunit. *EMBO J.* 10:1817–1825.
33. Lolis, E., and R. Bucala. 2003. Therapeutic approaches to innate immunity: severe sepsis and septic shock. *Nat. Rev. Drug Discov.* 2:635–645.
34. Gibot, S., M.N. Kolopp-Sarda, M.C. Béné, A. Cravoisy, B. Levy, G. Faure, and P.E. Bollaert. 2004. Plasma level of a triggering receptor expressed on myeloid cells-1: its diagnostic accuracy in patients with suspected sepsis. *Ann. Intern. Med.* 141:9–15.